Recent advances in vacuum sciences and applications

2014 J. Phys. D: Appl. Phys. 47 153001

(http://iopscience.iop.org/0022-3727/47/15/153001)

OPEN ACCESS
IOP Publishing
Journal of Physics D: Applied Physics
J. Phys. D: Appl. Phys. **47** (2014) 153001 (23pp)
doi:10.1088/0022-3727/47/15/153001

Topical Review

Recent advances in vacuum sciences and applications

M Mozetič[1,2], K Ostrikov[1,3], D N Ruzic[1,4], D Curreli[1,4], U Cvelbar[1,2], A Vesel[1,2], G Primc[1,2], M Leisch[1,5], K Jousten[1,6], O B Malyshev[1,7], J H Hendricks[1,8], L Kövér[1,9], A Tagliaferro[1,10] O Conde[1,11], A J Silvestre[1,12], J Giapintzakis[1,13], M Buljan[1,14], N Radić[1,14], G Dražić[1,2], S Bernstorff[1,15], H Biederman[1,16], O Kylián[1,16], J Hanuš[1,16], S Miloševič[1,17], A Galtayries[1,18], P Dietrich[1,19], W Unger[1,19], M Lehocky[1,20], V Sedlarik[1,20], K Stana-Kleinschek[1,21], A Drmota-Petrič[1,22], J J Pireaux[1,23], J W Rogers[1,24] and M Anderle[1,25]

[1] International Union for Vacuum Science, Technique and Applications, Avenue de la Renaissance 30, B-1000 Brussels, Belgium
[2] Jozef Stefan Institute, Jamova cesta 39, 1000 Ljubljana, Slovenia
[3] CSIRO Materials Science and Engineering, PO Box 218, Lindfield NSW 2070, Australia
[4] 106B Nuclear Radiations Laboratory, University of Illinois, 104 S Wright St., Urbana, IL 61801, USA
[5] Institut für Festkörperphysik, Technische Universität Graz, Petersgasse 16, A-8010 Graz, Austria
[6] Section Vacuum Metrology, Physikalisch-Technische Bundesanstalt, Abbestr. 2–12, D-10587 Berlin, Germany
[7] ASTeC—Accelerator Science and Technology Centre, STFC Daresbury Laboratory, Warrington, Cheshire WA4 4AD, UK
[8] NIST, Thermodynamic Metrology Sensor Science Division, 100 Bureau Drive, Stop 8364 Gaithersburg, MD 20899–8364, USA
[9] Institute for Nuclear Research, Hungarian Academy of Sciences, 18/c Bem tér, H-4026 Debrecen, Hungary
[10] Polytechnic of Torino, Department of Applied Science and Technology, C.so Duca degli abruzzi 24, I-10129, Torino, Italy
[11] University of Lisbon, Faculty of Sciences, Campo Grande, 1749-016 Lisboa, Portugal
[12] Instituto Superior de Engenharia de Lisboa, 1959-007 Lisboa, Portugal
[13] University of Cyprus, Nanotechnology Research Center, Nicosia, 1678 Cyprus
[14] Ruđer Bošković Institute, Bijenička cesta 54, 10000 Zagreb, Croatia
[15] Elettra-Sincrotrone, Basovizza, Italy
[16] Charles University in Prague, Faculty of Mathematics and Physics, V Holešovičkách 2, 18000 Prague 8, Czech Republic
[17] Institute of Physics, Bijenička cesta 46, 10000, 10000 Zagreb, Croatia
[18] Laboratoire de Physico-Chimie des Surfaces, UMR CNRS 7045, Chimie ParisTech (ENSCP), 11 rue P et M Curie, F-75005 Paris, France
[19] Surface Analysis and Interfacial Chemistry, BAM Federal Institute for Materials Research and Testing, Unter den Eichen 44–46, D-12203 Berlin, Germany
[20] Centre of Polymer Systems, Tomas Bata University in Zlín, nám. T G Masaryka 5555, 760 01 Zlín, Czech Republic
[21] University of Maribor, Faculty of Mechanical Engineering, Institute of Engineering Materials and Design, Smetanova 17, 2000 Maribor, Slovenia
[22] Kolektor Group, R & D Department Vojkova ulica 10, 5280 Idrija, Slovenia
[23] Universite de Namur, Rue de Bruxelles 61, B-5000 Namur, Belgium
[24] Center for Advanced Energy Studies, Idaho National Laboratory, Idaho Falls, ID 83415–3560, USA
[25] Knowledge Department, Autonomous Province of Trento, Via Jacopo Acconcio 5, I-38122 Trento, Italy

E-mail: miran.mozetic@ijs.si

Received 4 September 2013, revised 25 November 2013
Accepted for publication 25 November 2013
Published 27 March 2014

Abstract

Recent advances in vacuum sciences and applications are reviewed. Novel optical interferometer cavity devices enable pressure measurements with ppm accuracy. The innovative dynamic vacuum standard allows for pressure measurements with temporal resolution of 2 ms. Vacuum issues in the construction of huge ultra-high vacuum devices worldwide are reviewed. Recent advances in surface science and thin films include new phenomena observed in electron transport near solid surfaces as well as novel results on the properties of carbon nanomaterials. Precise techniques for surface and thin-film characterization have been applied in the conservation technology of cultural heritage objects and recent advances in the characterization of biointerfaces are presented. The combination of various vacuum and atmospheric-pressure techniques enables an insight into the complex phenomena of protein and other biomolecule conformations on solid surfaces. Studying these phenomena at solid–liquid interfaces is regarded as the main issue in the development of alternative techniques for drug delivery, tissue engineering and thus the development of innovative techniques for curing cancer and cardiovascular diseases. A review on recent advances in plasma medicine is presented as well as novel hypotheses on cell apoptosis upon treatment with gaseous plasma. Finally, recent advances in plasma nanoscience are illustrated with several examples and a roadmap for future activities is presented.

Keywords: vacuum, surface, plasma, interface, nanoscience

(Some figures may appear in colour only in the online journal)

1. Introduction

Vacuum sciences have received wide recognition as a broad research field comprising applied surface science, biointerfaces, electronic materials, nanometre structures, plasma science, surface engineering, surface science, thin films and pure vacuum science. The aim of this review paper is to highlight recent advances in vacuum sciences. Pure vacuum science is focused on outgassing of materials used in vacuum systems, rarified gas dynamics with modelling of complex vacuum systems and vacuum metrology. New developments in electron transport near solid surfaces are reviewed. Progress in analysis of carbon-based nanostructures and applications of surface analytical methods in conservation technology of cultural heritage objects will be presented. The surface characterization of materials presenting biological and/or biochemical interfaces are of great interest for both academia and industry. Indeed, bioimplants, anti-fouling properties, biomedical or diagnostic devices are some of the emerging technologies and applications which need fundamental understanding and knowledge. Ultra-high vacuum (UHV)-based surface analytical tools are used extensively for research, development and quality control of such biointerfaces, as powerful and reference tools. A selection of examples is presented, focusing on chemical speciation and quantification of surface functional groups as well as their reactivity, combining XPS and ToF-SIMS measurements. The more challenging aspects in probing biointerfaces lie in *in situ* characterizations at the solid–liquid interface in atmospheric conditions: existing analytical methods are then coupled to improved or dedicated new techniques, resulting in new approaches and methodologies. Surface engineering deals with the materials science and technology of modifying and improving the surface properties of materials for protection in demanding contact conditions or aggressive environments, as well as designing different functionalities with respect to combination of electrical, optical, thermal, chemical, and biochemical responses, including adaptive and active control of functions. Current hot topics are the synthesis of multifunctional surfaces, including active and adaptive control, the design of interfaces, and implementation of modelling approaches based on density functional theory, molecular dynamics simulations, and finite element methods for materials development, as well as engineered multilayers and nanostructured coatings. Recent progress in thin films includes the growth of thin film on granulates and hollow microspheres, MAX phases, magnetic and oxide thin films, and nanostructured thin films. We also discuss carrier mobility in organic thin films, quantum dot (QD) self-assembly, and superlattices investigation using grazing incidence small angle x-ray scattering (GISAXS). Current hot topics in plasma science include plasma nanoscience and plasma biomedicine. Methods for improved hemocompatibility of cardiovascular implants and soaking capacity of wound dressings are presented. Hypotheses on selective destruction of bacteria on body tissues are introduced and a theory on propagation of plasma bullets created by pulsed atmospheric low-frequency discharges is enlightened. Pure vacuum science is focused on outgassing of materials used in vacuum systems, rarified gas dynamic with modelling of complex vacuum systems and vacuum metrology.

2. Vacuum systems modelling, outgassing and metrology

Vacuum Science is in general the physics and chemistry of surfaces. The fact that in vacuum the particle density on the

surface goes up to ten orders of magnitude higher than in the volume, means the processes on the surface of the wall material are decisive. The main research and developments in this field are thus documented in surface and applied surface science. The technological scope of pure vacuum science and technology is stimulated and forced by very large projects. Great impetus is coming from accelerators and in particular from the Large Hadron Collider (LHC) at CERN. This installation is the largest vacuum system in the world and the main goal was to establish extremely low pressure in the beam line to avoid collisions during the acceleration of particles. A key issue for vacuum science research was the study of the outgassing behaviour of materials. Among all technical alloys stainless steel (SS) is the construction material of choice. Its main advantages are: standard machining and welding techniques, it is non-magnetic and chemically inert. The most disadvantageous property of SS is the outgassing of hydrogen. Hydrogen remains an impurity (1–4 ppm) after the production process in this endothermic alloy and provides a permanent source of gases. Since this outgassing of H determines the ultimate pressure of an UHV system the reduction of the outgassing rate is essential. Among different treatments such as bakeout in inert and low hydrogen content atmosphere, formation of adlayers to suppress the rate, high temperature bakeout (thermal outgassing) in vacuum became the most efficient way to reduce hydrogen outgassing. Thermal outgassing and in general the cleaning techniques in accelerator applications and in the majority of UHV applications is largely well understood [1–4]. Unfortunately a considerable part of the research work is not published but is shared within the vacuum science community at meetings, workshops [5] and conferences.

The design of UHV and extreme-high vacuum (XHV) systems for particle accelerators has gained an additional flexibility with the CERN's invention of non-evaporable getter (NEG) coatings [6, 7], which are in the meantime widely used. These coatings have two main advantages: lower desorption yield compared to materials used for accelerator vacuum chambers such as SS, copper and aluminum, and the coating acts as a virtual vacuum pump of uniformly distributed pumping speed. Recent results demonstrate well that the NEG coated vacuum chamber, even non-activated, performs better than a baked SS chamber. Activated at 180 °C, the NEG coated vacuum chamber provides a two orders of magnitude lower pressure. Being saturated, the NEG coating can be re-activated by electron bombardment. It has been found that the NEG coating morphology is very important for its proper operation [8–11].

Although the thermal outgassing is the main source of gas in the majority of vacuum systems, there is a class of vacuum system where desorption is induced by energetic particle (photon, electrons, ions, etc) bombarding (or irradiating) the vacuum chamber walls. Often this induced (or stimulated) desorption is a dominant source of gas in a vacuum system. To study different surface treatment to reduce such induced desorption e.g., electron stimulated desorption (ESD) was used as evaluation experimental method [12, 13].

Besides the thermal outgassing, heavy ion-induced desorption from the inner wall is a limiting factor for beam lifetime in a number of large accelerator facilities such as RIHC in USA, LIER and LHC at CERN or FAIR in Germany. Desorption yields were studied for numerous materials and coatings bombarded with different ions of different charge state and different energies and are documented in [14–17].

Presently most of the research activities in vacuum science and technology are focused on the huge fusion project ITER. ITER is a large-scale scientific experiment that aims to demonstrate that it is possible to produce commercial energy from fusion. The scientific goal of the ITER project is to deliver ten times the power it consumes. From 50 MW of input power, the ITER machine is designed to produce 500 MW of fusion power. During its operational lifetime, ITER will test key technologies necessary for the next step: that it will be possible to capture fusion energy for commercial use.

The successful operation of ITER requires the largest, complex vacuum systems yet to be built. The vacuum spaces comprise the main tokamak chamber of approximately 1400 m^3 volume and base pressure about 10−6 Pa, the cryostat vacuum for thermal insulation of the superconducting coils (volume ∼8500 m^3, base pressure ∼10−4 Pa), four neutral beam injectors (total volume ∼600 m^3, base pressure ∼10−7 Pa) and auxiliary vacuums for diagnostic, radio frequency heating systems and cryogenic circuits [18].

The vacuum spaces on ITER are provided by a set of around 400 vacuum pumps of ten different technologies. These are serviced by a network of vacuum lines. All gasses with the potential of being radioactive are routed to the vacuum pumping room in the tritium plant building. Some vacuum spaces such as the cryostat and cryogenic guard vacuum systems are always kept segregated to avoid contamination. Other vacuum spaces such as the torus and neutral beam vessels are frequently connected and form part of the closed fuel cycle. The optimal design of the ITER vacuum system benefits from both a practical and theoretical understanding of gas dynamics over an extreme range of different conditions [19].

2.1. Rarefied gas dynamics

Rarefied gas dynamics became an important part of the design and modelling of large vacuum systems and microsystems [18, 20–22]. Great efforts were made, therefore, to develop numerical and analytical methods to calculate rarefied gas flows and describe them in appropriate reviews [23–26]. Since in practice, however, one deals more with gaseous mixtures than with a single gas, the mathematical modelling of transport phenomena in gaseous mixtures is one of the present activities [19]. Gaseous mixture flows are determined by more parameters than single-gas flows. Besides the parameters for gas rarefaction, pressure, and temperature, mixture flows depend upon the chemical composition and the species composing the mixture. As a result of these complexities, the computational effort to model gaseous mixture flows drastically increases in comparison to that of a single gas. Several theoretical approaches to numerical calculations of gaseous mixtures over the whole range of Knudsen numbers have been developed [27–38] and the validity tested in benchmark problems [39–41].

Rarified gas dynamics plays an important role in the development of new pumping concepts for Tritium in the ITER vacuum system. All hydrogen isotopes originating from the torus or the cryopumps, during regeneration, are first pumped by a cryogenic viscous flow compressor (CVC). The design of the CVC was first optimized by modelling the gas dynamics and in parallel building and testing prototypes. Modelling of the gas flowing into the pump and through the pre-cooler heat exchanger and freezing tubes was first performed with a computational fluid dynamics (CFD) code. To fully optimize, the CFD code needs to be combined with a direct simulation Monte Carlo (DSMC) method to cover this transition region [18].

Computational investigations of complex geometries of model cryopumps have been performed using rarified gas dynamics with DSMC method. Since the flow close to the cryopanels can be assumed free molecular due to low pressures, the capture coefficient of the cryopanels can be estimated by applying the test particle Monte Carlo method. Then, this information can be used as input data to the corresponding DSMC simulations [42]. Simulation of the true three-dimensional (3D) complex geometry of the model cryopump by the newly developed PROVAC3D Monte Carlo code shows in the free molecular regime that the numerical simulation results are in good agreement with the pumping speeds measured. This means that the test particle Monte Carlo simulations in free molecular flow can be used not only for the optimization of the pumping system but also for the supply of the input parameters necessary for the future DSMC in the full flow regime [43]. Significant increase in the performance of classical pumps such as turbomolecular pumps was also obtained by gas dynamic calculations [44].

2.2. Vacuum metrology

Research and development work in vacuum metrology is basically concentrated to national institutions of standardization. The National Institute of Standards and Technology (NIST) in USA and the Physikalisch-Technische Bundesanstalt (PTB) in Germany are particularly active in research.

The Physical Measurements Laboratory of NIST started an ambitious project in NIST's competitive Innovations in Measurement Science programme. The plan is to develop ultra-precise optical interferometer cavity devices for pressure standards that will be accurate to about 1.4 ppm and will at the same time provide a new method of realizing and disseminating temperature and length and to revolutionize the way to measure all three basic quantities [45]. Such devices—initially developed at the size of a small mailing tube—would find immediate applications in commercial aviation, semiconductor (SC) manufacturing, and military activities, and they would also eliminate persistent difficulties in pressure metrology. The pressure and temperature of a gas are directly related to its density. Gas density is, in turn, directly related to the refractivity of the gas. In the instrument the PML team plans to develop, the refractivity of ultra-pure helium gas will be determined by locking lasers to the resonances of a variable-length, multiple Fabry–Pérot (FP) cavity. An FP cavity is formed by careful alignment of two highly reflective mirrors at each end of an enclosure (figure 1). A laser is locked to an FP cavity by tuning its frequency such that an integer number of half-wavelengths fit between the mirrors.

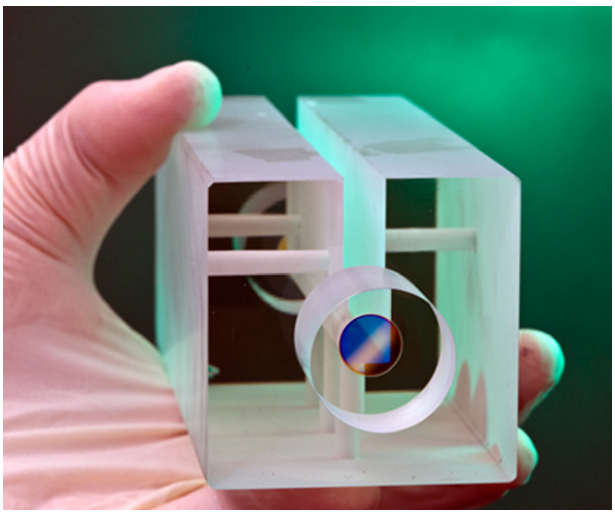

Figure 1. Glass enclosed ultra-precise optical interferometer cavity for prototype pressure device (figure courtesy of Jay Hendricks, NIST/PML Sensor Science Division).

In Europe, vacuum metrology has gained considerable revaluation by funding from the European Metrology Research Programme (EMRP) [46]. Since 2011 the vacuum sections of seven European National Metrology Institutes, supported by five industrial partners and three research grants, have worked together in the consortium EMRP IND 12 'vacuum metrology for production environments' to open up new measurement capabilities for vacuum and to help industry to characterize vacuum in industrial environments. In the first work package it is investigated how fast vacuum gauges can react on pressure changes in load locks or during fast processes. A dynamic vacuum standard was built where the pressure may change from 100 kPa to 100 Pa within 20 ms in a step-wise manner or within longer times up to 1 s in a predictable manner. To accomplish this, a gas expansion is carried out from a small chamber of 0.0001 m^3 at 100 kPa into a large chamber of 0.18 m^3 via an exchangeable duct. The expansion is initiated by a very fast opening gate valve which opens the full diameter within less than 5 ms [47]. The mass flow rate can be calculated by gas flow simulation software so that it is possible to predict the pressures and temperatures (figure 2) at any time in the small chamber. First experiments were performed with capacitance diaphragm gauges (CDGs) by INFICON, for which new electronics were developed so that a measurement signal is obtained every 0.7 ms with an output resolution of 21 bit (corresponds to 0.05 Pa for a CDG with full-scale 133 kPa). It was shown that the response time of these is certainly better than 2 ms which is the shortest time constant of the standard system [48]. The aim of the second work package is to improve the knowledge of gas flow through nano- and micro-channels in terms of predictability for different gas species and environmental conditions with the focus on the industrial applications and conditions. Extensive gas flow rate measurements for many

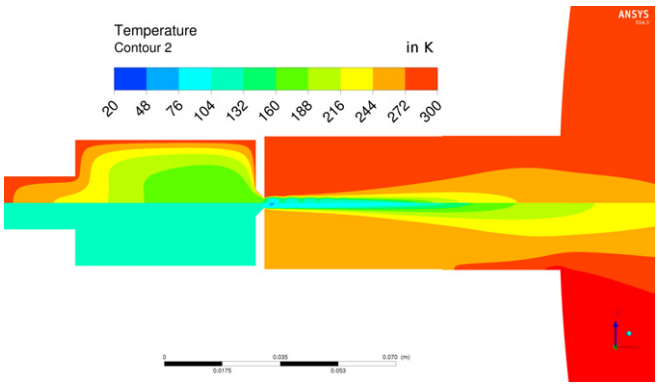

Figure 2. Cross sectional view of the temperature contours in the high pressure chamber *V 1* (left from small orifice) and in part of the downstream side chamber (right) as-received by ANSYS CFX ® in adiabatic (lower part) and isothermal boundary condition (upper part) at 200 ms after the beginning of expansion. In the adiabatic case the temperature in *V 1* is 110 K, while in the isothermal case the temperature in front of the orifice is 165 K. Reproduced with permission from [48]. Copyright 2014 Elsevier.

gas species and through elements such as focused ion beam produced holes with 200 nm diameter, laser drilled holes, specially prepared channels and fibres were carried out and are presently evaluated and compared with theory. In the third work package, dedicated calibration facilities for quadrupole mass spectrometers (QMSs) were developed and the factors influencing metrological characteristics of QMS are presently examined. A workshop was organized in April 2012 [49] to gather the latest information from manufacturers and key users of QMSs. The final goal is to develop a calibration procedure, together with the ISO TC 112 'Vacuum technology', which is useful for many users of QMS [50, 51]. In the same work package, traceability and standardized procedures for outgassing rate measurements will be developed as well. With EUV lithography the importance of traceable outgassing rate measurements has considerably increased, since all the components built into such facilities must be carefully checked in order not to affect the reflectivity of the x-ray mirrors. To this end the community has established the new term 'ultraclean vacuum' which characterizes a high-vacuum environment which is particle and hydrocarbon free.

The equivalence of eleven National Standards for leak calibrations was tested in an international comparison [52] for the first time. Two helium permeation leak elements of 4×10^{-11} mol s^{-1} (L1) and 8×10^{-14} mol s^{-1} (L2) were circulated and equivalence could be shown for most, but not all of the participating laboratories [53–56]. By this comparison, industrial laboratories for leak calibrations can be accredited and get international recognition of their certificates.

3. Surfaces, electron transport, carbon nanostructures

Applied surface science has recently become one of the most important fields of research stimulating the revolutionary changes in science and technology of our age. Below, examples for some of the latest remarkable achievements are reviewed briefly in three selected subsections: 3.1. Electron transport near solid surfaces; 3.2. Surface analysis of carbon-based nanostructures; 3.3. Applications of surface analytical methods in conservation technology of properties of cultural heritage.

3.1. New developments in electron transport near solid surfaces

Novel methods, elaborated for describing accurately near-surface energy loss processes and simulating electron, photon and ion-induced electron spectra have predicted new phenomena during surface excitations, as confirmed later by experiments. Applications of these methods for interpretation of electron spectra reveal unknown details of electronic structure of new materials of great practical importance. The upper part of figure 3 shows a process called the supersurface scattering, not identified before in experimental electron backscattering spectra or in related simulations [57]. As a consequence of the surface plasmon excitation in vacuum near an Au surface by the incoming or outgoing electrons, their energy and direction is changing slightly, leading to large changes in the probability of electron backscattering near the deep minima in the differential elastic scattering cross section (DECS) versus scattering angle curve (lower part of figure 3). This phenomenon results in strong oscillations of the angular dependence of the surface excitation probability in vacuum side of the solid and these oscillations are anti-correlated with the changes in the DECS as a function of the scattering angle. The experimental data well reproduce the predictions of simulations accounting for angular deflection of electrons moving in vacuum near the surface [57]. Posing new challenges to the present assumptions on the surface excitation parameter, this is the first direct observation of surface plasmon excitations by an electron moving in vacuum near surface.

Compared to the case when a photoelectron travels in an infinite solid, the presence of the ionized atom (with a suddenly created core hole) left behind and the surface (surface excitations at surface crossings of the emitted photoelectrons) influence (decrease) the intensity of the photoelectrons emitted from a solid. Pauly and Tougaard used the dielectric response model for describing the combined effects of the core hole and the surface [58]. Figure 4 shows the parameter CP_{XPS} accounting for the attenuation of the XPS peak intensity as a function of the emission angle (with respect to the surface normal), for different energy photoelectrons, in the case of Si [58].

3.2. Progress in analysis of carbon-based nanostructures

Complex application of surface analytical methods for studying chemical and structural properties of doped or functionalized carbon nanotubes (CNTs) or graphene layers lead to the development and production of new, highly effective catalysts of important chemical reactions, as well as to further exciting novel applications of these nanostructures in science and technology. Multiwalled carbon nanotubes (MWCNTs), due to their (or their modified forms') unique physical and chemical properties are very interesting materials for applications of great significance e.g., as supports for metallic catalysts used in electro-oxidation reaction in fuel cells or

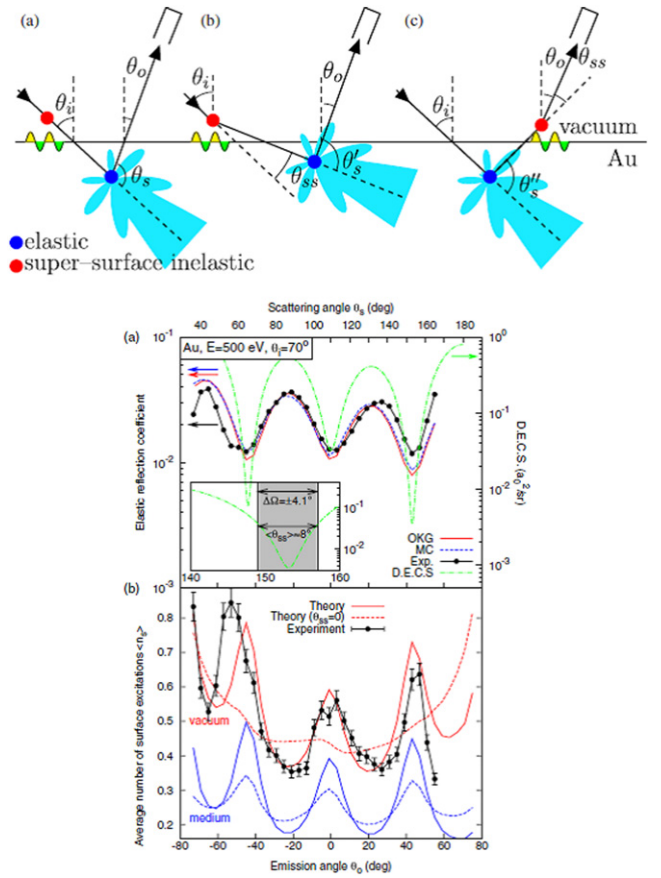

Figure 3. Upper part of the figure: supersurface electron scattering without (*a*) and with (*b*) and (*c*) deflections (θ_{ss}) caused by inelastic interaction (surface excitation) of the incoming (*a*) and (*b*) and the outgoing (backscattered) electrons near the surface of a solid. Lower part of the figure; (*a*) intensity of 500 eV energy electrons (70° angle of primary beam incidence) backscattered elastically from Au surface, as a function of the scattering angle. The solid curve with data points shows the measured elastic peak intensity (normalized to theory at 80° scattering angle), the solid and dashed curves the elastic peak intensity using the Oswald–Kasper–Gaukler [59] and the Monte Carlo models, respectively, the dashed–dotted curves the differential cross section for elastic electron scattering (the expanded view of the region in the scattering angle range between 140° and 160°, shown in the inset is compared with the input solid angle of the electron energy analyser and the average angle of deflections in the supersurface process). Lower part of the figure; (*b*) Average number of surface excitations (absolute units) as a function of electron emission angle. The solid curve with data points shows the experimental values, the dashed and solid curves the values calculated using Monte Carlo simulations without and with accounting for deflections due to surface excitations, respectively. The curves in the upper part of (*b*) are related to the surface excitations while the electrons move in vacuum, the curves in the lower part of (*b*) to the surface excitations while the electrons move inside the solid. Reproduced with permission from [57]. Copyright 2013 American Physical Society.

utilized for gas storage. Before modifications, however, the synthesized MWCNTs need to be purified, removing all contaminations (amorphous carbon, traces of catalysts and catalyst's support, defects, etc). Stobinski *et al* [60] elaborated a process for wet chemical purification, oxidation and functionalization of MWCNTs studying the original and oxidized MWCNTs using transmission electron microscopy

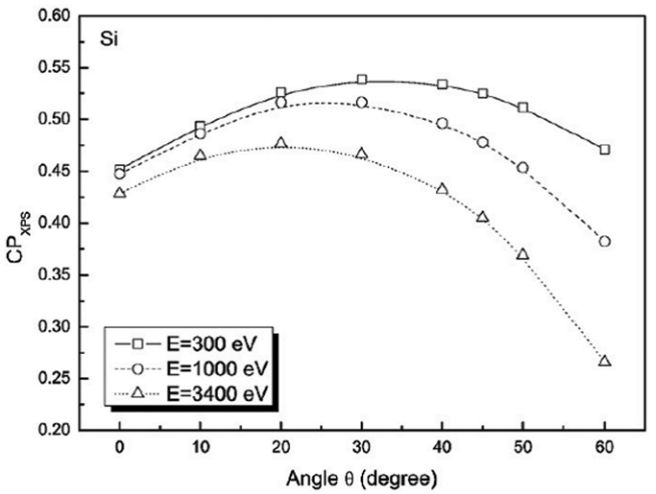

Figure 4. The parameter CP_{XPS} accounting for the reduction of the XPS peak intensity—as a consequence of the effect of the core hole left behind and the effect of surface excitations at surface crossing of the photoelectrons—as a function of the emission angle (with respect to the surface normal), for different energy photoelectrons, in the case of Si. Reproduced with permission from [58]. Copyright 2010 Elsevier.

(TEM), scanning electron microscopy (SEM), elemental analysis, mass spectrometry, EDX, FTIR, Raman and electron spectroscopic methods (XPS, EPES, EELS, REELS) [60]. It was shown from the consistent results of this complex analysis that the proposed wet chemical purification and modification method effectively removes all impurities originating from the procedure of synthesizing the MWCNTs [60]. The surface sensitivity of the electron spectroscopic methods proved to be greatly helpful in determining quantitatively the surface properties, such as the surface chemical composition of the 'as-received' or modified MWCNTs or in determining the content of the C sp^2 and C sp^3 bonds from the first derivative [61] of the C KLL Auger spectra [60]. Electron spectroscopic studies of structural and chemical properties of Pd/MWCNTs catalysts used for fuel cell applications led to the identification of the main reason of the deactivation of these catalysts, namely the formation of poisons from the impurities of the formic acid, especially the carbonaceous overlayer developing on the Pd surfaces [62].

In the case of various polymers the combined application of electron spectroscopic methods (EPES, REELS, XPS) and the pattern recognition method to study effects of electron induced degradation resulted in the consistent identification of phenomena as decreasing content of hydrogen and increasing the C sp^2 bond content during irradiation [63]. These studies provide information on the stability of different polymers against electron induced degradation as well [63].

Graphene structures are in the focus of the frontline research nowadays because of their unique physical properties and the strong hope to witness soon a spectacular increase of their various important practical applications. In the case of graphene grown on Cu(1 1 1) substrates by thermal chemical vapour deposition of carbon from methane, Tapasztó *et al* observed nanometre-wavelength rippling of graphene suspended over nanotrenches of the Cu substrates [64].

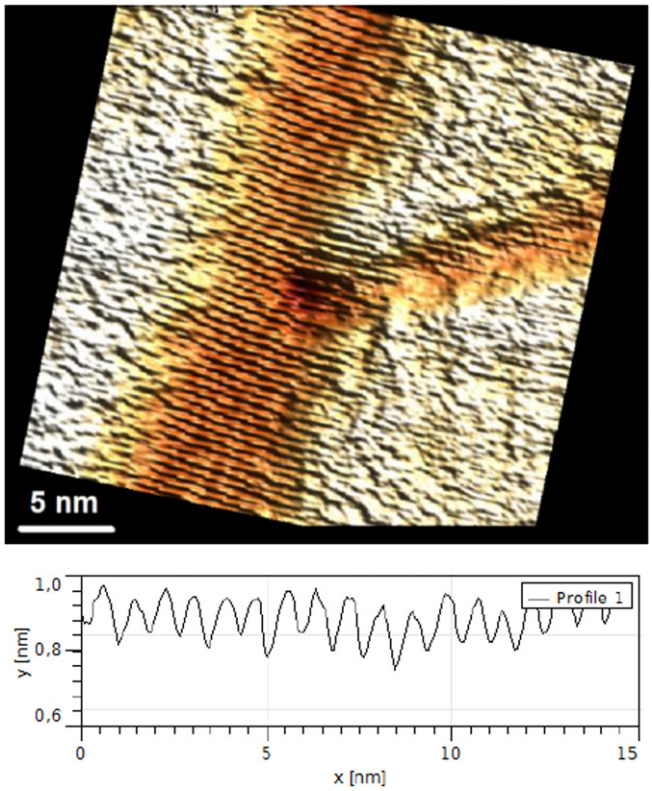

Figure 5. Upper part: STM image of a graphene membrane suspended over a 10 nm wide nanotrench of the Cu(1 1 1) substrate, displaying the characteristic graphene ripples. Lower part: STM line scan showing the magnitude of the ripples. Reproduced with permission from [64]. Copyright 2012 Nature.

Figure 5 shows the STM image (upper part) of a graphene membrane suspended over a 10 nm wide nanotrench of the Cu(1 1 1) substrate, displaying the characteristic sub-nanometre graphene ripples and the STM line scan (lower part) showing the magnitude of the ripples [64]. Continuum mechanics cannot describe these nano-ripples and Tapasztó *et al* used a microscopic force model based on density functional theory with tight-binding approximation for the successful interpretation of the ripples [64]. This result—the controllable production of the electric superlattice in graphene—has a fundamental significance for the nano-electro-mechanic systems (NEMSs) based on graphene [64].

4. Conservation technology of cultural heritage objects

The number of applications of surface and interface analytical methods in studies of archaeological objects and conservation technology of cultural heritage is steadily increasing. An important field of applications is the study of deteriorating environmental effects—including biodeterioration, bio-degradation and weathering—on cultural heritage artefacts. Because the surface region of cultural heritage objects can be very complex and heterogeneous, for characterizing the nature, structure and composition of these materials, in most cases a combination of complementary analytical methods are needed. Below, some examples of

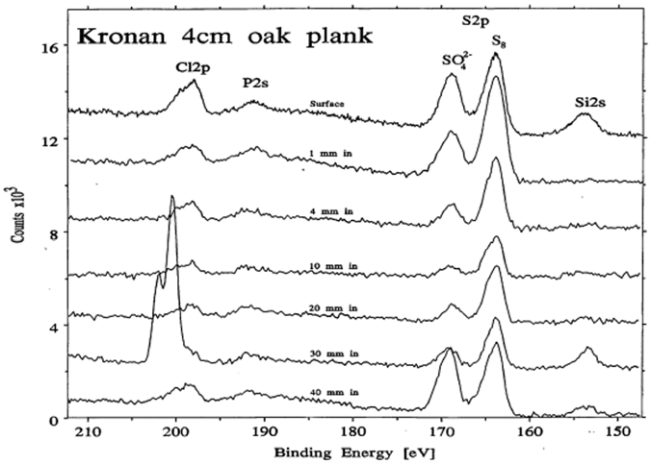

Figure 6. XPS spectra of regions along an oak core taken from the orlop deck of the shipwreck of the warship Kronan sank in the Baltic Sea in 1676 during a battle. The spectra show the presence of the dominating reduced ('S_8') and the oxidized ('SO_4^{2-}') forms of sulfur (the quantity of the latter is increasing close to the surfaces) and the presence of the silicon, chloride and phosphate in the core. Reproduced with permission from [68]. Copyright 2012 Elsevier.

applications of surface analytical methods for studies and conservation of mosaics, ancient wall paintings and wooden objects are mentioned.

Mosaics of the Roman Villa del Casale near Piazza Armerina (Sicily, Italy) were studied using a combination of a number of techniques (SEM-EDX, XRD, XPS, UV–VIS–NIR reflectance, optical microscope, colourometry) [65]. The study revealed not only the chemical composition and degradation state of the tesserae, but provided information on the procedure of their fabrication and their origin as well [65]. Surface and bulk techniques, such as XPS, XRF, XRD, laser induced breakdown spectroscopy and ionic chromatography were used for characterizing pieces from the wall matrix sampled at different depths when investigating the degradation of the walls with medieval graffiti in the Chiaramonte Palace in Palermo [66]. Soluble salts were found as the major degradation agents of the porous matrixes studied and in order to avoid salt crystallization and deterioration of graffiti, in addition to de-sulfating and desalination treatments, first a very high (higher, than 85%) humidity was proposed to be maintained [66].

Application of combined surface and bulk analytical methods proved to be very important for improving conservation technology of historical wooden objects as ancient wrecks of battleships buried under the sea [67]. Combined and extended XRD, XAS, XANES, XPS, FTIR, NMR, MALDI-TOF mass spectrometry, chromatography and optical analyses were performed and the presence of iron compounds and a very high amount of sulfur in different oxidation states in addition to elemental sulfur was shown, threatening the ships with the danger of large-scale deterioration after recovering [67]. These studies made clear that iron acted as a catalyst of sulfur oxidation and the origin of sulfur was attributable to the activity of bacteria living in the deep sea and converting the sulfate content pollution into hydrogen sulfide that penetrated into the wooden parts of the ships [67]. Figure 6 shows XPS spectra taken

along an oak core cut from the orlop deck of the ancient shipwreck of the warship Kronan sank in the Baltic Sea [68]. The spectra indicate the presence of the dominating reduced ('S_8') and the oxidized ('SO_4^{2-}') forms of sulfur (the quantity of the latter is increasing close to the surfaces) and the presence of the silicon, chloride and phosphate in the core. These results stimulated further and more detailed research of deteriorating and conservation processes in the case of shipwrecks, including studies of wooden materials exposed to simulated environments [67, 68] and on the basis of the analytical results and model experiments, new procedures were proposed for safe long-term conservation of waterlogged wood objects.

5. Biological and biochemical interfaces

The surface characterization of materials presenting biological and/or biochemical interfaces (i.e. biointerfaces) are of great interest for both academia and industry. Indeed, implants, biomedical or diagnostic devices, biotechnology, personal care, food production, anti-fouling properties, are some of the emerging technologies and applications which need fundamental understanding and knowledge.

However, experimental techniques which reveal the details of the solid–liquid processes provide limited information and, in many cases, do not provide information that may be interpreted in a reliable and quantitative manner. Within this field, many practitioners rely upon the use of vacuum-based methods to understand the nature of the interface before and after events have taken place within a liquid. Thus, UHV-based surface analytical tools are used extensively for research, development and quality control of such biointerfaces, as powerful and reference tools. The importance of this field has been recognized within IUVSTA with the inauguration of the Biointerfaces division.

Another point is that the theme of biointerfaces is transversal and multidisciplinary, thus there is a general consensus that access to historical studies and data is difficult and presents a significant barrier for new researchers in the area. The main issues appear to be that the earliest works are hard to find using modern databases due to patchy coverage; recent studies are published in a wide range of journals and are of a variable quality. Providing the link between surfaces, characterizations and UHV, a dedicated issue of the *Surface Science* journal published a series of reviews of great interest [69].

Where, what and how many are fundamental questions which must be systematically answered with regard to the adsorbed biomolecules. A selection of examples will be presented, focusing on chemical speciation and quantification of surface functional groups as well as their reactivity, combining XPS and ToF-SIMS measurements.

5.1. Biointerfaces for diagnostic and medical applications

Personalized medicine and point of care (POC) diagnostics are fields of tremendously growing importance in the recent society. Devices developed for personalized medicine and POC often make use of interfaces engineered on a (bio-) molecular level. Proper function can be only reached when these interfaces are carefully characterized enabling optimization and trouble shooting. An example of a type of diagnostic device used for personalized medicine and POC is a microarray. Successful microarrays require careful characterization of the interfaces between supports (i.e. glass or polymer slides), the linker molecule and the attached biomaterial used as probe on the one hand, and between the probe and target biomolecules on the other hand. For real medical applications and clinical use, biosensors like microarrays have to go through an approval process under control of regulatory authorities (e.g., FDA) in order to guarantee reproducible, reliable and repeatable performance.

A thorough physical–chemical characterization of biointerfaces by surface chemical analysis is of great benefit for a deeper understanding of what really happens at the interfaces mentioned above and to get proper control on them. Such studies result in a more rational design and further optimization in terms of sensitivity and specificity of biosensing devices. Specifically, microarrays represent a sensor system in the field of medical diagnostics that allows simultaneous screening of a wide range of biomarkers in a patient's serum or other bio matrices using a single chip. Diagnostic microarrays are highly relevant multiplex or high-throughput diagnostic devices.

DNA or oligonucleotide arrays are often prepared on amino-terminated supports either by selective covalent binding to the amino (NH_2) groups or by unspecific UV cross-linking of the oligonucleotides to the support material. Amino surfaces can be obtained from a number of different vendors. XPS analysis of such slides demonstrated that the chemical species on the surface might be rather different from that intended and the final performance achieved by a microarray thereon will therefore be less than ideal [70].

From the highly resolved N 1s core-level XP spectra, the amount of NH_2 moieties can be determined. In the same way, the amounts of other nitrogen-containing species can be determined as well and this kind of information is rather useful for quality assessments because only free amines (and NH_3^+) can be used for the immobilization reactions in the next step of microarray production. The amide component at a binding energy of 400 eV in the N 1s XP spectrum is rather useful as an indicator of aging due to oxidation [71–73]. Besides amide, various other species hampering a reproducible DNA attachment can be present on the surface, e.g., amine, imine, oximes, nitrile, etc, but identified by XPS and ToF-SIMS as well. The amount of free amino groups may reach fractions >90% as shown by XPS and ToF-SIMS on freshly prepared amino-modified model surfaces [70, 74].

Besides aminated supports, epoxy slides enjoy great popularity for microarray applications due to their broad reactivity towards various functional groups as thiols, amines and alcohols. Immobilization of many different classes of biomolecules is enabled in this case. Recently successful quantification of reactive epoxy surface groups was demonstrated in a combined XPS and fluorescence approach using Rhodamine 110 as a dye [75]. On-going research is done to use that dual XPS-fluorescence label approach for quantification of other reactive surface groups, for example, amino groups, using a custom-made Bodipy dye [76].

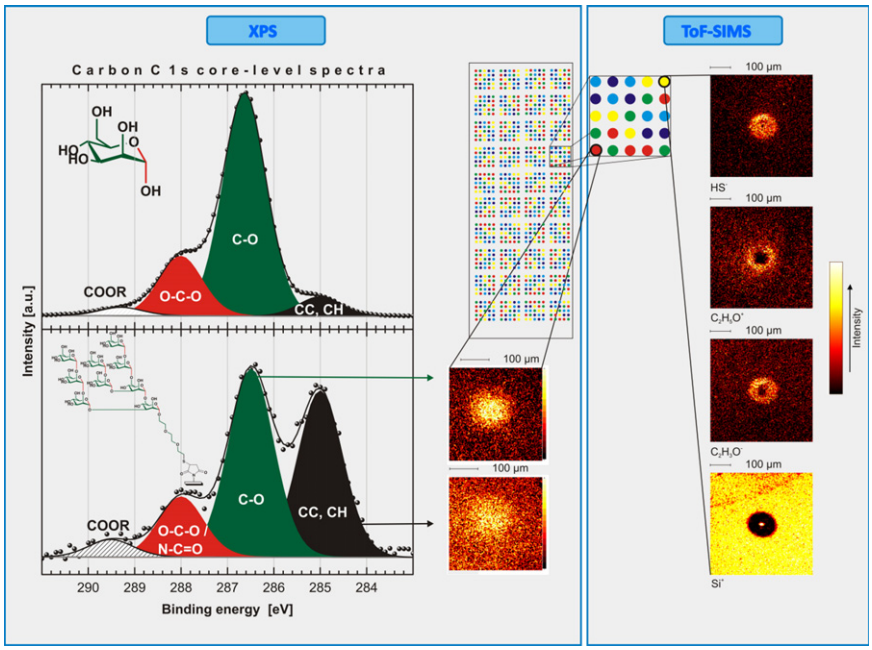

Figure 7. Left column: comparison of highly resolved C 1s XPS spectra of a simple carbohydrate, mannose, and a more complex oligosaccharide measured in a microarray spot (∼100 μm diameter) printed on a maleimide-functionalized glass slide. Two XPS images of a single spot are shown using the binding energies of C–O (carbohydrate specific) and CC, C–H species. Right column: ToF-SIMS images of oligosaccharide (HS^-, $C_2H_3OH^-$, $C_2H_5O^+$) and substrate (Si^+) specific secondary ions [78, 79].

Other relevant microarrays are based on carbohydrate-based interactions. Especially for clinical diagnostics, these so-called glycan microarrays play a vital role because carbohydrate-based interactions are involved in many recognition events in a living cell. So it is a challenge for surface chemical analysis to characterize the specific surface chemistry of immobilized sugar molecules on glycan microarrays. For example, a microarray prototype prepared in Seeberger's group was analysed by XPS and ToF-SIMS with a view to establish its detailed surface chemistry. A model surface using a dimannose-thiol self-assembled monolayer (SAM) on gold was prepared in order to identify specific spectral signatures in XPS and ToF-SIMS, which are useful to characterize relevant chemical moieties present on biointerfaces at glycan microarrays [77–79]. Surface chemical analysis by XPS and ToF-SIMS was successfully used to identify and quantify relevant chemical species existing on the glycan microarray (figure 7). High-resolution C 1s XPS of the printed arrays showed component peaks of carbohydrate-specific acetal and C–O moieties allowing imaging and quantification of immobilized carbohydrates in single spots. In ToF-SIMS fragment, ions relevant for sugar have been found, and the HS^- fragment is useful for monitoring the reaction of sugar with the maleimide-functionalized glass slide. Homogeneity issues for a single spot can be successfully identified by XPS and ToF-SIMS imaging in a label-free manner (figure 7).

In a more fundamental approach, simple and versatile design of oligoethylene based SAM using thiolene chemistry, starting from commercially available compounds, and providing high-quality SAM exhibiting adhesive and anti-adhesive patterns, have been demonstrated on metal oxide surfaces: on silicon oxides (and particularly glass substrate for cell biology applications) but also on biocompatible metals such as titanium [80].

XPS and ToF-SIMS allow getting chemical fingerprints of the reaction at each step, depending on the selection of the oligoethylene glycol (figure 8). The C 1s core-level spectra indicate that, in the first step, a robust vinyl-terminated surface (C, C–H species) was obtained (*a*), in a second step, the adhesive O-(2-Carboxyethyl)-O′-(2-mercaptoethyl) heptaethylene glycol has reacted (*b*) to the previous surface (new O–C–O, C–O bonds). ToF-SIMS spectra (*d*) and images (*e*) and (*f*) of a vinyl/heptaethylene glycol pattern reflect the chemical grafting according to a 100 μm-large mask (yellow bands correspond to oligoethylene-terminated surface, through its specific marker $C_2H_3O^-$).

5.2. Combining UHV and in situ characterizations at the solid–liquid interface

The more challenging aspects in probing biointerfaces lie in *in situ* characterizations at the solid–liquid interface, at atmospheric pressure: it is possible with current and emerging techniques to measure the identity, amount and structure of adsorbates at solid–liquid interfaces. A wide range of methods are available which have varying levels of maturity and sophistication. The development of new and emerging methods is hampered by the lack of benchmarks which are both useful and easy to employ. Radiolabelling is widely considered to be the most acceptable benchmark method and has the advantage that it is accurate, if the correct procedures are used (see [81] for example). However, the capabilities and expertise to perform such measurements are not widespread and difficult to compare to other methods on the same samples due to the issue of instrument contamination with radioactive material.

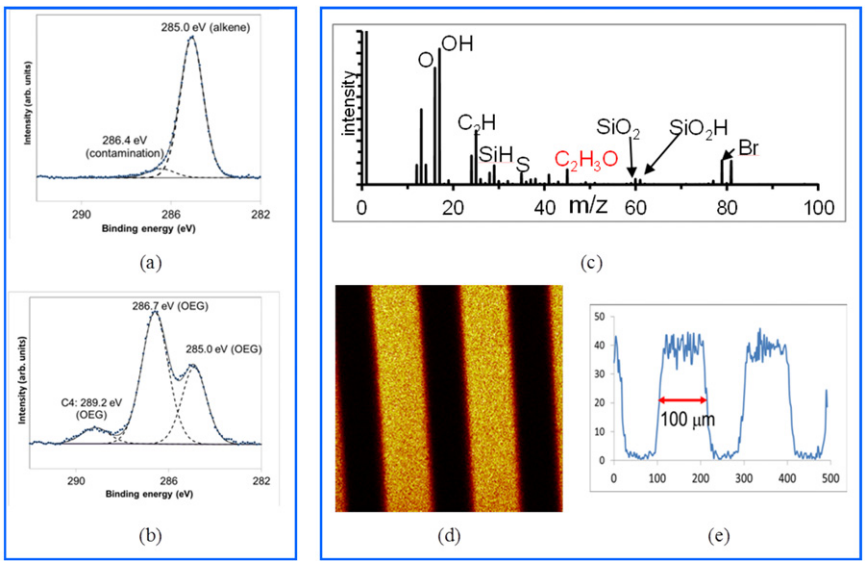

Figure 8. Left column: comparison of highly resolved C 1s XPS spectra of a silicon surface treated by undecenyltrichlorosilane (*a*) and O-(2-Carboxyethyl)-O′-(2-mercaptoethyl) heptaethylene glycol activated by N-hydroxysuccinimide (OEG) (*b*). Right column: ToF-SIMS spectrum of negative ions (*c*) following the thiolene reaction step (*b*) enlighting $C_2H_3O^-$, specific marker of OEG. ToF-SIMS image of the vinyl-terminated/OEG-terminated pattern ($C_2H_3O^-$) showing sharp and regular 100 μm-large bands (*d*) and (*e*) [80].

The sensitivity and reproducibility of other methods, such as quartz crystal microbalance (QCM) and optical techniques (surface plasmon resonance (SPR) [82], ellipsometry) are good but their accuracy is less certain and they have a narrower applicability. Additionally, the practical implementation of the various techniques contributed to a lack of comparability. Equally important in this regard is the availability of materials or systems where adsorption behaviour is known, well understood and reproducible. By XPS, it is possible to follow peptide or protein adsorption from the careful examination of the C 1s and N 1s core levels: the shape of the XP peaks may be used to describe the surface modification, while relative intensities are used to measure adsorbed amounts of protein either as equivalent continuous and homogeneous layers [83–86], or as a surface coverage of islands of proteins (infinite heights) [87, 88]. By combining XPS to QCM quantitative measurements, it allows a chemical macroscopic description of the protein adsorption, tested as a function of *in situ* (mass uptake) changes (or as a function of time of interaction). With two quantitative techniques, it is possible to use a more sophisticated model, as proposed in [81], where the adsorbed amounts are islands of proteins, quantified by their height and surface coverage. However, great care must be taken to establish the accuracy and comparability of the techniques and understand what factors contribute to each of the measurements, for example the amount of uncoupled water that contributes to the QCM measurement [86]. For example, in the frame of cleaning of protein BSA-contaminated Ti or Cr surfaces by sodium dodecyl sulfate (SDS), it was possible to detect *in situ* and real-time uptake of BSA on the clean surface, then partial desorption by SDS (at 37 °C) on Ti, and further sequences of new BSA uptake and partial cleaning by SDS. This desorption does not occur with a solution of buffer (PBS) only (figure 9). In the same conditions, a different behaviour of the Cr surface was observed: SDS adsorbs partially reversibly without removing adsorbed BSA [89]. The data describing

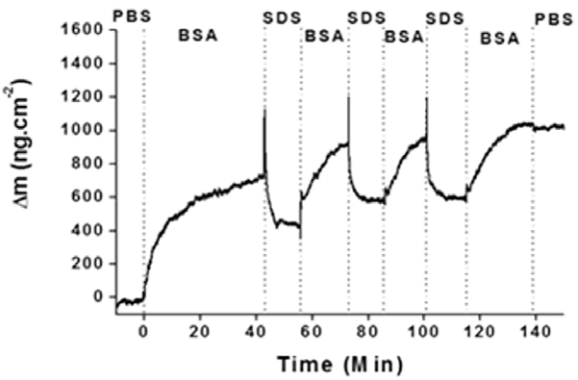

Figure 9. Mass variation versus time for a Ti quartz crystal. The experiment was performed at OCP and at 37 °C. The vertical dashed lines indicate switches between solutions: pure phosphate buffer saline (PBS, 0.01M), BSA (20 mg L-1 in PBS), SDS 0.09 M [89].

the adsorption of BSA, as obtained from the combination of XPS and QCM results also differ: BSA adsorbs on Cr with a surface coverage of 0.7 ± 0.2, with island heights of 5 ± 1 nm, close to a full monolayer coverage of denatured protein, while BSA adsorbs on Ti with a lower surface coverage of $0.4 \pm 0{,}2$, with island heights of 13 ± 3 nm [85], keeping more reactive functions towards the surfactant. The different behaviour in surface cleaning may be attributed to different modes of initial BSA adsorption. It is thus possible to efficiently probe biointerfaces by UHV and *in situ* characterization techniques. It is interesting to couple the existing analytical methods to improved or dedicated new techniques, resulting in more and more reliable new approaches and methodologies.

6. Thin films and carrier mobility

Most techniques for the production of thin films require either a preliminary vacuum to tackle contamination issues (as in

chemical deposition techniques [90]) and/or an appropriate vacuum level during deposition (as in a number of physical deposition techniques [91]). The existence of vacuum system can hence somewhat be considered the base brick of the field of thin films growth. This field encompasses a wide range of materials and application. Thin films are for instance used to realize x-ray mirrors [92]. In the early days of thin-film technology the coating of curved substrates was a tough challenge but nowadays it is possible to coat even granular materials [93]. In more recent years, the type of materials deposited in thin-film forms and investigated has been steadily increasing. In some cases they have peculiar properties that barely have a counterpart in the bulk case. For instance, organic thin films can be manipulated to obtain high electrical conductivity values [94] and hence become candidates for electronic applications. Another example is given by MAX phases. Their layered structure allows obtaining systems having conduction properties like metals and mechanical ones like ceramics [95]. The field of thin film is so huge that we cannot offer more than a glimpse in this short review. In the following we will just offer a few examples of current on-going research in the field.

6.1. Magnetic oxide-based thin films

Aiming to achieve a new type of information technology with improved performance, lower energy consumption, and/or entirely new functionalities, spin-based electronics or spintronics seeks to incorporate the spin degree of freedom into the conventional charge-based electronics. The initial development of spintronics was based on the success of magnetoresistive devices, especially giant magnetoresistive and tunnelling magnetoresistive devices, which are composed primarily of ferromagnetic (FM) metallic multilayers [96]. Materials that exhibit large carrier spin-polarization at the Fermi level, such as the half-metals Fe_3O_4 and CrO_2, can dramatically enhance device performance.

SC spintronics is the next stage in the development of spintronics technology, for which the design of materials combining both semiconducting and FM properties turns out to be of crucial importance [97]. The development of magnetic SCs should allow easier integrability with the existing SC technology and would be vital to allow signal amplification with highly spin-polarized carriers. Among the oxide-based diluted magnetic semiconductor (DMOS) materials with potential use in the development of spintronics devices, Co-doped TiO_2 and SnO_2 have attracted particular interest due to their reported FM behaviour well above room temperature (RT) for low Co doping concentrations.

Here we present results on the growth of $Fe_{3-x}O_4$ thin films on p-type Si(1 0 0), having a native SiO_2 layer of $\approx$2 nm, using pulsed laser deposition (PLD). During deposition the substrate temperature was kept at 210 °C and the total pressure was 8.0×10^{-2} Pa. High quality, polycrystalline films consisting of randomly oriented crystallites with $x = 0.01$ and uniform thicknesses between 100 and 400 nm were obtained [98]. Saturation magnetization values of 490 emu cm^{-3} and coercivities of 40 mT were achieved at RT. More interestingly, these films display a large power factor of 70 mW K^{-2} m^{-1}, attributed to tunnelling of electrons from the Fe_3O_4 into an accumulation layer of holes located at the Si/SiO_2 interface [99]. Therefore, these Fe_3O_4/SiO_2/p-type Si(1 0 0) heterostructures are potential candidates for thermoelectric applications beyond their conventional interest for spintronics.

The PLD technique was further used to grow the aforementioned DMOS systems. Pure rutile and anatase Co-doped TiO_2 thin films, as well as films with a mixture of both polymorphic phases, were grown by non-reactive PLD using argon as buffer gas, onto sapphire substrates heated at 310 °C, by varying only the working pressure [100]. Epitaxial rutile films formed at PT $=$ 7 Pa while pure anatase ones were grown at PT $\geqslant$ 60 Pa. Polycrystalline films with rutile-anatase mixture of phases were obtained at 20–60 Pa, the anatase content increasing with increasing PT. The microstructure of the films strongly depends on their phase composition. Films consisting predominantly of anatase show a porous microstructure that could be particularly attractive for applications requiring materials with large specific surface areas. Optical band gaps are red shifted for all samples in comparison to the values usually reported for undoped TiO_2, which is related with the introduction of electronic states by the 3d electrons of Co_2^+ cations and oxygen vacancies, and therefore with n-type doping of the TiO_2 matrix. The increase of the band gap red shift as the working pressure decreases is consistent with the corresponding increase of the Urbach energy. The narrowed band gaps bring the absorption edge of Co-doped TiO_2 films into the near-visible region, in relation with the phase composition of the films, which suggests that non-reactive PLD with variation of only the working pressure could provide a method for band gap engineering in the near-visible region. For the SnO_2 based DMOS [101], the Co doping resulted in an optical band gap blue shift that could be explained by the Burstein–Moss effect. Further co-doping with Mo, reverted this tendency most probably due to the higher oxidation state of Mo compared to Sn. For the Co and Mo doping concentrations investigated, the presence of Mo did not contribute to increase the conductivity of the films or to enhance the FM order of the Co-doped films.

6.2. Self-assembled growth of Ge QDs in Ge/Al_2O_3 multilayers

Production processes of regularly ordered 3D lattices of QDs are important because nano-based materials which contain such lattices are widely used in many relevant nanotechnology applications [102–104]. An interesting new route for the production of such materials was developed recently using a magnetron sputtering deposition [105, 106]. SC (Ge) clusters embedded in dielectric amorphous matrices such as SiO_2 and Al_2O_3 were produced using that technique. It has been shown there that surface morphology mechanism and diffusion mediated nucleation drive the self-assembly process during the growth of such films [105]. The self-assembly mechanism of Ge QDs was investigated in mixed ($Ge^+Al_2O_3$)/Al_2O_3 multilayers [106, 107]. In this system, the resulting 3D Ge QD lattices have body-centred tetragonal (BCT) structure,

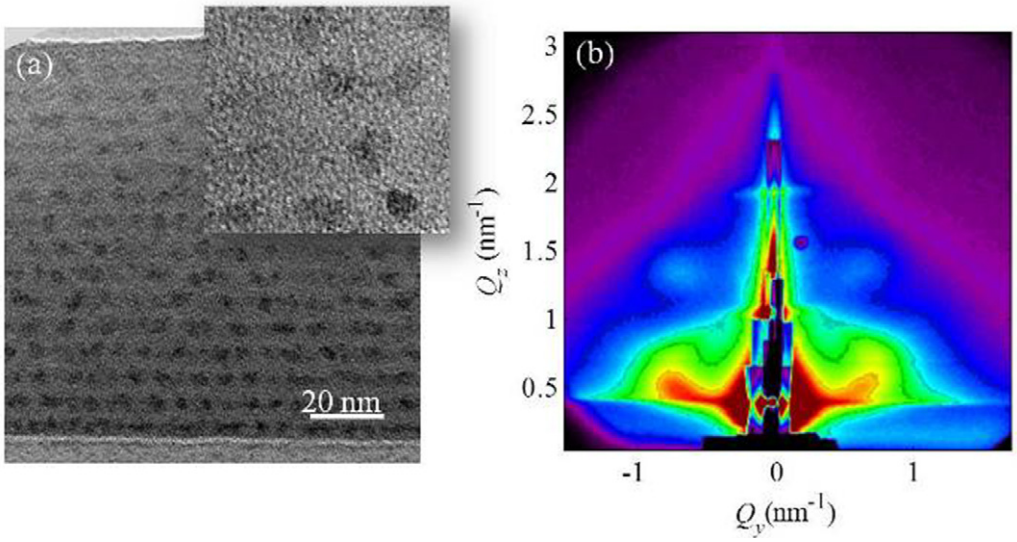

Figure 10. (*a*) TEM image of the Ge/Al_2O_3 film and (*b*) the corresponding GISAXS map. The inset shows TEM image with better resolution.

and they consist of nearly spherical Ge QDs which are fully surrounded by an alumina matrix. Here we present the investigation of self-assembly of Ge QDs in the pure Ge/Al_2O_3 multilayers. For that purpose 20 alternating Ge and Al_2O_3 layers were deposited by dc and RF magnetrons operating at 8 W and 300 W, respectively. The working pressure of Ar was 4 mbar, and the substrate temperature was 300 °C during the deposition.

The structural properties of the film were investigated by TEM and GISAXS. The experimental details of the measurement techniques can be found in [106]. TEM images of the film and the corresponding GISAXS map are shown in figures 10(*a*) and (*b*), respectively. From the TEM images it follows that the formed Ge QDs are nearly spherical and also well separated by alumina matrix like for the case of $Ge^+Al_2O_3$ deposition. The internal structure of the formed Ge clusters is amorphous (see the inset of figure 10(*a*)), as is the standard case for the deposition of Ge clusters in alumina [106]. Some regularity in the QD ordering is also visible in the TEM images. However, the QD ordering is much better observed by GISAXS technique where intensity maxima appear due to the correlation in the QD positions [108]. Four such maxima can be resolved in the GISAXS map of the film (figure 10(*b*)). Their arrangement is the same as for the case of the mixed layers which are investigated in [106] showing the same ordering type of the QDs (BCT QD lattice). The quality of ordering is also excellent as follows from the narrow Bragg peaks visible in the GISAXS map. The same quality of ordering was found for the mixed films. Such ordering properties clearly demonstrate formation of Ge islands on alumina substrate during the deposition. The nucleation positions of such islands are determined by the positions of the surface minima in the alumina layer. The next alumina layer fully covers the formed Ge islands and determines the nucleation positions for the following Ge layer. In that way, the self-assembly process is the same as for the case of the deposition of mixed $Ge^+Al_2O_3$ layer. In summary, it has been shown that the well separated Ge QDs form during the deposition of Ge/Al_2O_3 multilayer stuck. Moreover, the same ordering type of Ge QDs as for the case of the mixed $Ge^+Al_2O_3$ layer deposition was found.

6.3. Production and use of nanoclusters to tailor thin-film properties

Due to their unique properties, nanoclusters and nanoparticles are attracting increasing attention. One possible method of producing nanoparticles is to use gas aggregation sources (GASs). In these sources a material is evaporated into a relatively high pressure of inert gas (∼10–100 Pa) and nanoparticles are created by homogeneous nucleation. This occurs in an aggregation chamber. Nanoparticles are then dragged by the buffer gas and exit the aggregation chamber through an orifice into a deposition chamber. This concept was modified by replacement of an evaporator with a planar magnetron [109], which enabled the production of nanoparticles from materials that have high melting point temperatures. GAS systems were commonly equipped with mass filters to produce nanoparticles with very narrow size distributions. However, the use of these systems is hampered by low deposition rates and by the necessity to use costly ultra-high-vacuum systems. Therefore, simplified high-vacuum GAS systems that do not use mass filtration (e.g., [110–112]) were introduced. These systems, schematically depicted in figure 11, consist of a water cooled aggregation chamber terminated with a conical orifice (1–2 mm in diameter). Inside the aggregation chamber a dc planar magnetron equipped with a metallic target (2 or 3 inch in diameter) is placed. The whole setup is attached to a deposition chamber. By means of this GAS different metal nanoparticles were produced (e.g., Ag, Au, Cu, Ti presented in figure 11). Moreover it was shown, that it is also possible to produce plasma polymerized nanoparticles when the dc magnetron is replaced by an RF magnetron equipped with a polymeric target [113, 114].

A key advantage of GAS is the possibility to combine them with other vacuum-based deposition systems

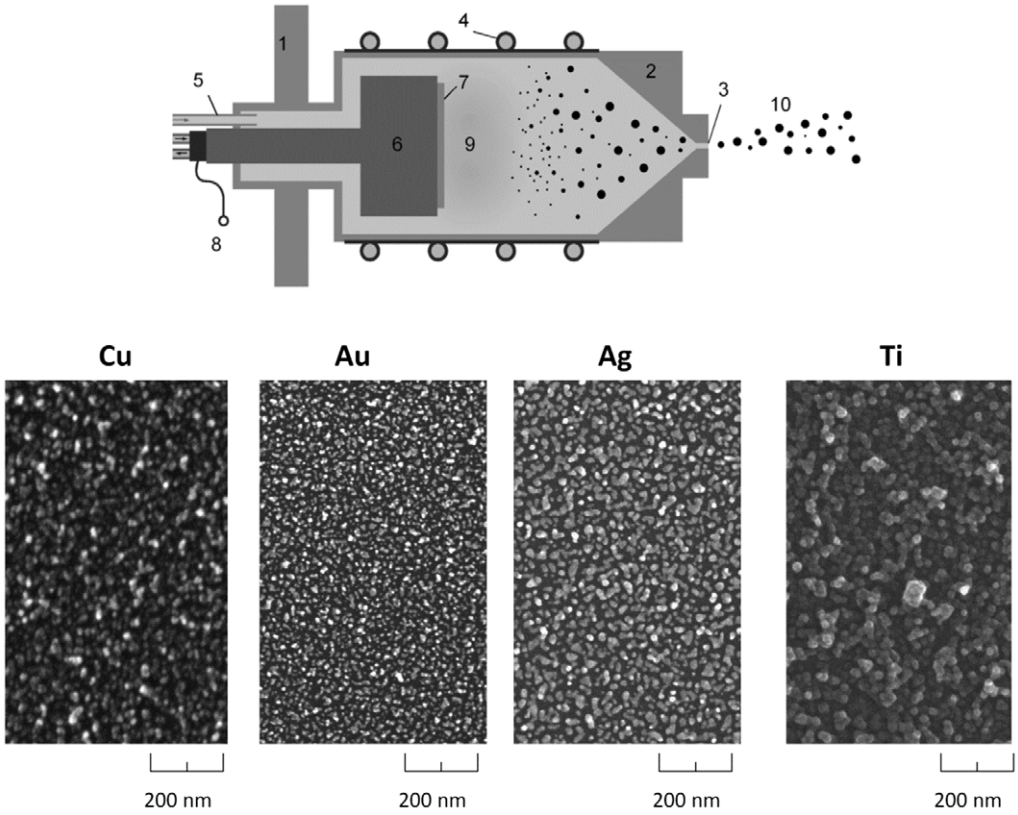

Figure 11. Gas aggregation nanocluster source (1-vacuum flange, 2-aggregation chamber, 3-exit orifice, 4-water cooling, 5-gas inlet, 6-magnetron, 7-target, 8-electrical connection, 9-plasma, 10-beam of nanoparticles) and sections of SEM images of produced films of Cu, Au, Ag and Ti nanoparticles. Reproduced from [110]. Copyright 2012 Elsevier.

(e.g., plasma-enhanced chemical vapour deposition (PECVD) or magnetron sputtering). This allows effective production of nanocomposite materials in one deposition chamber. An example of this is deposition of Ag/C : H coatings by simultaneous deposition of Ag nanoparticles and a C : H matrix [110]. It was shown that the nanoparticles produced by GAS may also be used for control of surface roughness. In this case a two-step process that consists of a deposition of a film of nanoparticles onto a smooth surface followed by overcoating of this film by a thin overlayer with desired chemical composition was suggested. This method enables independent control of the surface roughness and chemical composition of the resulting coatings [115]. The chemical composition of the surface is given solely by the overcoat material, while the surface roughness may be adjusted either by the sizes or by the number of nanoparticles deposited in the first step. This approach has already been employed for tailoring surface wettability [115] and for preparation of nanorough titanium substrates for investigation of the role of surface roughness on the growth of osteoblast-like cells [116].

7. Plasma nanoscience

Synthesis and processing of nanomaterials is another area where vacuum plasma technologies find numerous applications. The range of pressures used in these applications varies from fractions of mTorr to multiples of atmospheric pressure. This broad range of process operating pressures makes it possible to control the production of reactive species, the degree of thermal and chemical non-equilibrium, the role of collisions and several other factors that determine the specific outcomes of the envisaged nanoscale processes. Research in plasma nanoscience helps identifying the most relevant plasma-specific effects that enable control of the nucleation, growth and post-processing (e.g., functionalization) of numerous nanoscale objects [117–120]. These objects span all three dimensions and can be made of a very broad range of materials systems with diverse functional properties. The structure and morphology of these materials can be tailored by the plasma processes and these materials can be tailored to feature metallic, dielectric, or semiconducting properties, be opaque or transparent to electromagnetic radiation in specific frequency ranges, etc. In this section we briefly overview the key features of the plasma effects in the synthesis of the common nanomaterials that typically require low and intermediate gas pressures. These nanomaterials are represented here by zero-dimensional QDs, one-dimensional (1D) nanotubes and nanowires, two-dimensional (2D) graphenes and 3D nanocones. We also focus on the most typical materials systems, such as carbon-, silicon-, oxide- and nitride-based nanostructures.

7.1. Carbon nanotubes

Since the pioneering discovery of MWCNTs in arc-discharge plasmas [121], a very large number of publications have

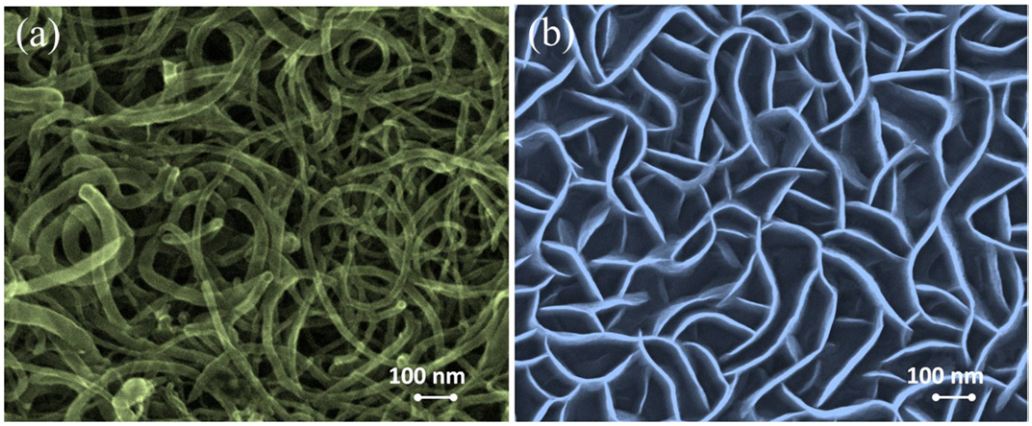

Figure 12. SEM micrograph of entangled network of plasma synthesized MWCNT (*a*) and elongated carbon nanowalls (*b*) with spacing around 100 nm which were synthesized in $CH_4 + H_2$ plasma gas mixture. Courtesy of Filipič G, Slobodian P, Tajima S, Kondo H, Sakine M, Hori M and Cvelbar U (unpublished).

reported on the successful applications of low-temperature, low (e.g., tens of mTorr) and intermediate-pressure (e.g., ∼1–10 Torr) plasmas of hydrocarbon precursors for the synthesis and functionalization of single- and MWCNTs (figure 12). These successful applications and the plasma effects involved have recently been critically reviewed [122]. Vertical alignment of the nanotubes along the direction of the electric field within the plasma sheath is perhaps one of the most prominent plasma-specific effects which was reported and explained in the late 1990s to early 2000s [123, 124]. It is presently possible to effectively control the growth rates, alignment, density, size distribution, etc of the CNTs by synergistically using the plasma and catalyst nanoparticle effects. Most recent advances include the demonstration of the effective control of size (and to some extent, chirality) distribution of single-walled CNTs (SWCNTs) [125, 126] and the possibility to avoid using catalyst and to directly integrate CNTs into the presently dominant Si-based nanodevice platform [127]. Several open questions remain, in particular, on the role of nanoscale interactions of the plasma with metal catalyst that contribute to the SWCNT chirality selection [128] and the possibility of additional early growth stages of CNTs that are strongly affected by the plasma (e.g., etching) effects [129].

7.2. Carbon nanotips and related structures

A variety of plasma-based techniques (e.g., plasma-enhanced hot-filament-based, PECVD, etc) have been used to produce carbon nanotips and related structures (e.g. carbon nanofibres, CNFs) with a variety of morphological and structural properties [130, 131]. These properties can be effectively controlled by adjusting the discharge power and pressure, which in particular affect the ion focusing by the nanostructures [132]. Thermal effects that arise through both the ion collisions with the surface and through the recombination of reactive species on the surface play a major role, and are very different compared to similar processes conducted at atmospheric pressures. Although a variety of self-organized 3D patterns of carbon nanocones and other nanostructures have been reported, it still remains challenging to produce regular and ordered arrays without pre-patterning or pattern delineation. The mechanisms of such self-organization related e.g., to the gas pressure and electric charge effects also await their conclusive interpretation. Apart from traditional applications in electron field-emitting devices, other applications, e.g., in optoelectronic devices with tunable photoluminescence are being pursued.

7.3. Graphenes

Graphene and related nanomaterials have recently been in the spotlight of a diverse range of studies and applications because of their highly unusual electrical, optical, and mechanical properties. These properties can be tuned by controlling the number of graphene layers and defects in the structure. A further flexibility can be achieved by arranging graphenes vertically, which makes it possible to more effectively use open reactive edges [133]. Low-temperature plasmas have been used to grow and process both horizontal and vertical configurations of graphenes. The most common processes include catalyst-assisted growth [134], etching of reactive edges to produce graphene nanoribbons [135], reversible hydrogenation to produce graphene, a bent hydrogenated analogue of graphene [136], as well as to reduce graphene oxide (GO) to graphene, doping to control the bandgap and some others.

The open questions include the ability to control damage (e.g., due to ion bombardment) to atomically thin graphene sheets, intentional creation of defects to control functionality of graphene, thinning vertical graphenes to ultimately single-atom thin graphene, maximizing the effects due to the open reactive edges, effective transfer of graphene sheets from the catalyst to devices, as well as exploring environment-friendly synthesis options using natural precursors [137].

7.4. Nanowires

Inorganic nanowires have been successfully grown under vacuum or low-pressure conditions for numerous years [138]. The primary interest for nanowires is in energy harvesting

and energy conversion devices such as photo-electrochemical cells. The important shift was recently made from catalyst supported to directly grown nanowires, where the nanowires are grown from their own nuclei synthesized by plasma at the first growth stage [139, 140]. The competitive advantage of plasma grown nanowires against thermally or wet-chemically grown nanowires is the speed of their synthesis [141] as well as crystallinity and pureness with the absence of residual atoms left by catalyst or growth medium. [142] Over the last several years many different types of metallic oxide nanowires [143–145], nitride nanowires [146, 147], Ge and Si nanowires [148–150], and alloyed nanowires [151] have been successfully synthesized. As realized in numerous experiments, the nanowire growth and morphology can be precisely controlled by control of discharge and plasma parameters. Controlling the gas flow, composition of gas mixture, discharge power, partial pressure, surface temperature, etc, enables the control of nanowire morphologies such as thicknesses or surface densities. However, these discharge parameters are just intermediate factors for plasma parameters (particle densities, energies, densities of surface charge, surface potential, etc) which enable nanoscale chemistry of plasma species during interaction with surfaces [152]. By controlling ion and neutral fluxes, surface charge, supply and demand of plasma building units and surface recombination, we can practically grow any nanowire type in arrays or just as a single-crystalline nanowire. An advantage of plasma processing is also surface doping or material-type conversion. The typical example is a conversion of metallic oxide nanowires to nitrides or sulfites by slow domain substitution [153]. An extra conversion can be done as well with electron beam irradiation, where we can reduce the number of atoms in the crystal structure and transform oxide into metallic [154]. Moreover, significant progress has been made in the field of fast processing and achieving high yields of nanowires—production of kilogram quantities per hour at low pressure as well as at atmospheric-pressure conditions, which might lead to wider implementation of advanced material into devices [155].

7.5. Quantum dots

The smallest versions of nanomaterial synthesized in plasmas are QDs. These QDs are the smallest mono-crystalline materials, which could be used to trap light photons and improve efficiency of solar cells. The plasma proposed concept is either grow QD particles inside the plasma from building units or at the surface. If we consider growth inside the plasma, we have to control size and structure of nanoparticles through plasma gas phase building units which depend on the leaking gas [156] or on plasma neutrals/ions species ratios [157]. However, we have to consider control of particle agglomeration, transport and sticking. In such plasma 'nano-factory', nanocrystalline Si particles of desired size can be synthesized [158, 159]. Moreover, the single-crystalline dots can also be modified during deposition in order to change their structure. One of the more interesting processes is nitridation of Si nanoparticles in SiH_4/H_2 mixture with N_2,

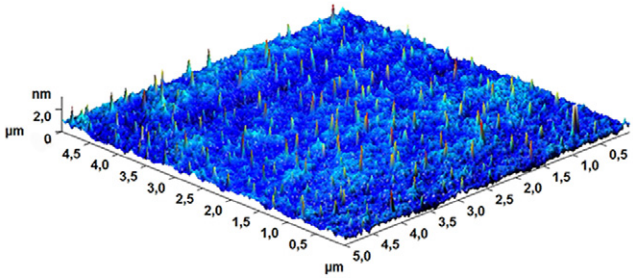

Figure 13. AFM image of plasma synthesized SiO_2 nanodots on Si surface. Courtesy of Modic M and Cvelbar U (unpublished).

which improves the photon-to-current efficiency to 40% at a short wavelength of 350 nm [160]. Alternative to plasma-in synthesis and deposition of QDs to surface is direct synthesis on surfaces via phase transformation mechanisms, where surface recombination and other surface properties influence synthesis of QDs. An example of such synthesis are SiO_2 QDs on Si wafer surface, where single Si atoms undergo phase transformation with impinging plasma oxygen atoms, agglomerate and rearrange on the surface (figure 13) [161].

8. Plasma biomedicine

Treatment of biomedical materials by gaseous plasma has an enormous potential in future applications. While sterilization of delicate materials which do not stand autoclaving has been elaborated in the past decade there are still open issues mainly concerned with interaction of reactive plasma particles with materials themselves. It is a generally accepted theory that both UV radiation from plasma as well as chemical interaction between reactive gaseous particles and bacteria or spores cause damage to bacteria. Unfortunately, it has been also shown that delicate materials such as polymers are not immune to reactive gaseous particles. Best results were obtained using oxygen-containing gas for plasma sterilization but reactive oxygen particles cause not only functionalization of polymer surface but slow etching as well. The etching could be minimized by avoiding interaction with gaseous ions using flowing afterglows for sterilization but slow etching was observed even in late afterglows [162]. Happily enough, the etching rate for a typical polymer used for manufacturing delicate medical devices is orders of magnitude smaller than corresponding rates for bacterial capsule, cell wall or cytoplasm destruction. Application of late oxygen plasma afterglows is useful not only for bacterial destruction but also for gentle removal of bacterial cell wall, thus revealing the structure of cytoplasm. In fact, treatment of certain bacteria revealed rigid structure of cytoplasm which is a direct evidence of the existence of cytoskeleton [163]. The major task for future research in the field of plasma sterilization is application of plasma with parameters that are suitable for destruction of bacteria but cause only marginal damage to the materials which are to be sterilized.

The major groups of diseases which are currently not cured satisfactorily include neurodegenerative and cardiovascular diseases as well as diabetes and cancer. Ageing of population

reflects in increasing rate of neurodegenerative diseases such as dementia. A particular problem to be solved is early diagnosis of such diseases before visible symptoms are evident. The neurodegenerative diseases are due to existence of certain proteins in body liquids including cerebrospinal liquid and blood. The concentration of these proteins is extremely low and thus difficult to detect. A particular problem arises from the fact that the proteins tend to adsorb on surfaces including the Eppendorf tubes used for storage of body fluids. Recently, great progress in preventing the proteins adsorption on the tubes was reported [164]. The inner walls of Eppendorf tubes are first treated by helium plasma created by a low-pressure RF discharge in the capacitive mode. The treatment allows for surface activation which is favoured for anchoring protective coatings. The right mixture of thin films containing specific chemicals allows for negligible adsorption of the proteins in storage tubes [165]. An open issue in this field remains long-term stability of coatings since the samples should be stored for a rather long time before being thoroughly characterized.

Cardiovascular diseases are often cured by surgery. A bad blood vessel is replaced with an artificial one made from a polymer—typically PET or PTFE. While such vascular grafts perform well as long as they are of large diameter, their biocompatibility is insufficient for small diameters below several millimetres. The rather poor biocompatibility is reflected in activation of plod platelets, release of factors and enzymes, surface agglomeration of modified blood proteins and finally formation of a thrombus. If this happens the surgery should be repeated. One way of preventing this effect is deposition of anti-coagulant coatings [166] or various nanoparticles [167]. Another possibility is modification of vascular grafts using highly non-equilibrium oxygen plasma [168]. As already mentioned, polymers are slowly etched upon exposure to oxygen plasma. The etching with highly non-equilibrium oxygen plasma with large concentration of neutral oxygen atoms is often inhomogeneous, so the surface of treated polymers gains nanostructured morphology [169]. Such a morphology when combined with the presence of highly polar functional groups leads to super-hydrophilic character of the polymer surface. Such an effect prevents activation of blood platelets when incubated with platelet-rich human blood plasma [170]. While this effect is not yet fully understood the most probable hypothesis drawn on the basis of the experimental results and surface characterization is that the blood proteins conformation on the plasma treated surfaces differ from the conformation on untreated surfaces [171]. Furthermore, the nanostructured morphology prevents substantial contact with a blood platelet, thus preventing its activation. The activation is reflected in a dramatic change of the platelet shape. While inactivated platelets are of almost spherical shape a well activated platelet assumes a highly spread form, as shown in figure 14. Imaging of the platelets' shapes and counting the number of platelets in different shapes therefore allows for quantitative determination of the activation rate. Oxygen plasma treatment allows for a decrease of fully spread platelets after prolonged incubation for more than three orders of magnitude when compared to untreated vascular grafts. These results are therefore encouraging but an open

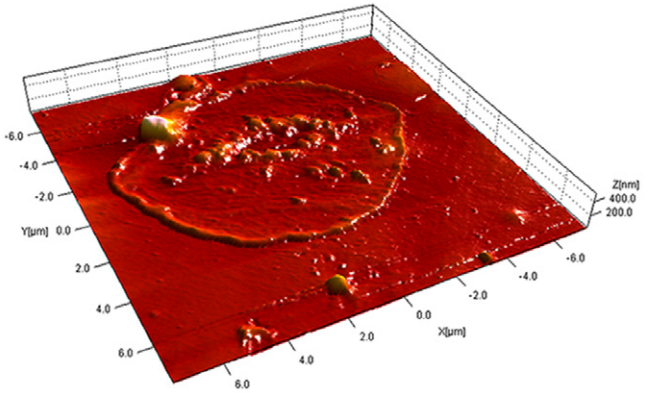

Figure 14. AFM image of a fully spread well activated human blood platelet. Courtesy of Modic M (unpublished).

question in this field remains any toxicity of plasma treated materials for vascular grafts and ability of endothelization, i.e. formation of uniformly distributed and dense endothelial cells on the inner surface of the vascular grafts after implanting.

Diabetes is another burning problem of modern society. The diabetes wounds are notorious for curing. Once a wound appears and develops it becomes chronic and curing easily lasts several months if not longer. In order to facilitate curing of such wounds, plasma techniques are applied either to modify materials used for wound healing or to treat the wounds themselves. Low-pressure discharges are used in the first case, while only atmospheric ones are suitable in the second one. The sorption properties of currently used materials for diabetes wound healing are far from optimal. Currently, non-woven cellulose materials are used as the absorption layer. Other materials like alginate have much better sorption properties but they are also much more expensive and since the curing lasts for months the cost of wound dressings would be prohibitively high. As mentioned above, plasma treatment allows for surface activation as well as nano-structuring of polymer materials and both effects lead to improved sorption properties. A definite drawback of plasma technology when applied for treatment of porous materials is poor penetration of reactive plasma particles into the bulk material. Namely, the particles tend to neutralize, thermalize, de-excite and recombine on the surfaces of solid materials so their concentration inside a porous material is very low. The problem of neutralization of charged particles could only be solved by establishing a strong electric field across the porous material but such a field will cause formation of too aggressive plasma and the material will burn. Happily enough, the polymer materials will be activated and weakly etched also by using neutral reactive particles, such as neutral oxygen atoms in the ground state. The only problem with such plasma radicals is loss by heterogeneous surface recombination. This problem is overcome by pumping neutral oxygen atoms through the porous absorption layer of wound dressings [172]. A pressure gradient across the material to be functionalized is established so the atoms do not have to diffuse inside the porous material but rather drift. Such a configuration allows for deep and uniform functionalization of extremely porous materials [173]. The effectiveness of passing oxygen atoms through non-woven cellulose material for wound

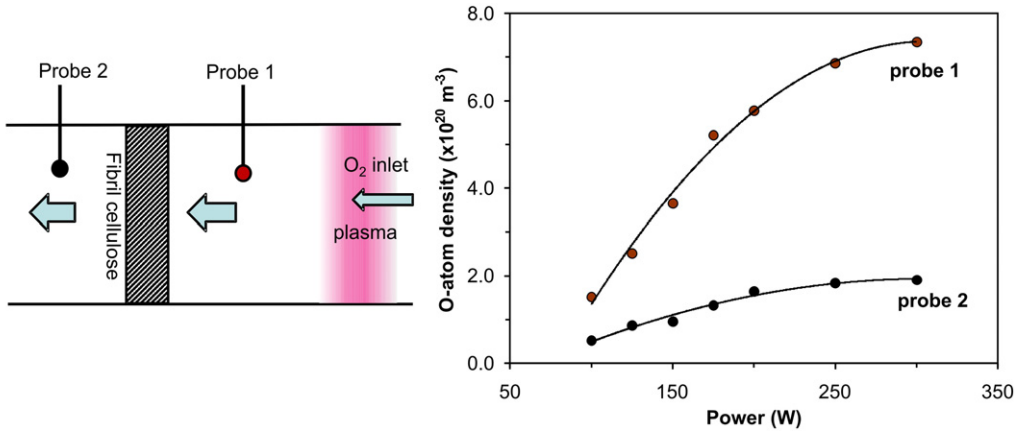

Figure 15. Schematic of the experimental setup for deep functionalization of porous materials and the oxygen atoms density on both sides of the non-woven cellulose sample. Courtesy of Mozetic M, Vesel A, Persin Z and Stana-Kleinschek K (unpublished).

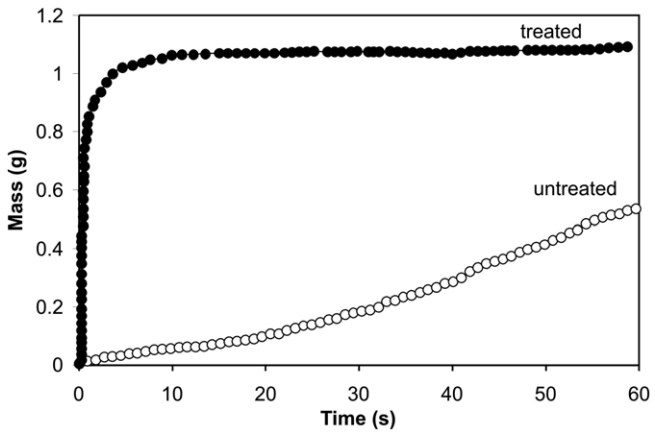

Figure 16. Sorption of exudate by untreated (solid curve) and plasma treated (dashed curve) non-woven cellulose sample. Courtesy of Mozetic M, Vesel A, Persin Z and Stana-Kleinschek K (unpublished).

dressing is confirmed by measuring the neutral atom density in the gas phase on both sides of the sample. Figure 15 represents a schematic of the experimental system and measured values of oxygen atom density as determined from catalytic probes signals. The result of such deep activation is dramatic improve of the sorption rate for exudate, as shown in figure 16. As in many other cases of plasma modified materials, the ageing problem may be severe since materials are often used months after performing plasma treatment.

The application of cold non-thermal atmospheric-pressure plasmas has proven to be of high potential for applications in dermatology [174] for the direct treatment of wounds. Differently from thermal plasmas, cold plasmas can be conveniently used on heat-sensitive surfaces like the mammalian skin, retaining a number of unique features of atmospheric-pressure plasma discharges such as the delivery of reactive species, UV light, high electric fields and energetic ions. Laboratory studies indicate that direct plasma treatments can improve wound healing by reducing bacterial colonization and by a direct action on epidermal cells [174]. Clinical tests have shown that a significant reduction up to 35% in the bacterial load leads to an accelerated wound healing. Plasma acts on the wound also as a haemostatic agent, favouring the coagulation of blood [175]. An argon plasma coagulation method [176–181], originally patented in 1977 [182], has been in use for the past decade as a non-contact method of electro-coagulation, with special applications for gastrointestinal endoscopy. The use of atmospheric-pressure plasmas extends also to cosmetic treatments, such as skin rejuvenation and treatment of wrinkles, approved in 2005 by the US Food and Drug Administration.

9. Selective destruction of bacteria on body tissues

The high bactericidal effect of plasmas, known for a long time but reported for the first time in 1996 [183], can conveniently be used for the selective destruction of bacteria on body tissues, even without harming living mammalian cells. Numerous *in vitro* studies [184–194] have proven that cold atmospheric-pressure plasmas can effectively inactivate and kill bacteria placed on a Petri dish. Figure 17 shows atomic force microscopy images of a plasma treatment on *Bacillus cereus*, a bacteria genetically similar to *Bacillus anthracis*, in a time sequence starting from untreated conditions, and after 2, 4 and 8 s of plasma exposure. The laboratory studies opened the way to further investigations on the selective destruction of on bacteria on living tissues. A number of new plasma devices have been developed, ranging from dielectric barrier discharges (DBDs), plasma pencils, plasma bullets and non-thermal floating-electrode DBDs [195] using the living tissue as a second active floating electrode.

The application of an external electric field on living cells has a well-known porative effect on the cell phospholipid membrane [197]. In first approximation, cells electrically behave as a conductive volume surrounded by a dielectric membrane. The application of a low electric field polarizes the cell; when a current is run, the accumulation of electric charges on the cell membrane generates a potential difference across the membrane. Above a critical voltage, the dielectric membrane reconfigures itself opening nanopores. The pores allow the forced extraction/introduction of material from/into the cells. One of the possible mechanisms of selective necrosis of prokaryotes (bacteria) on eukaryotes

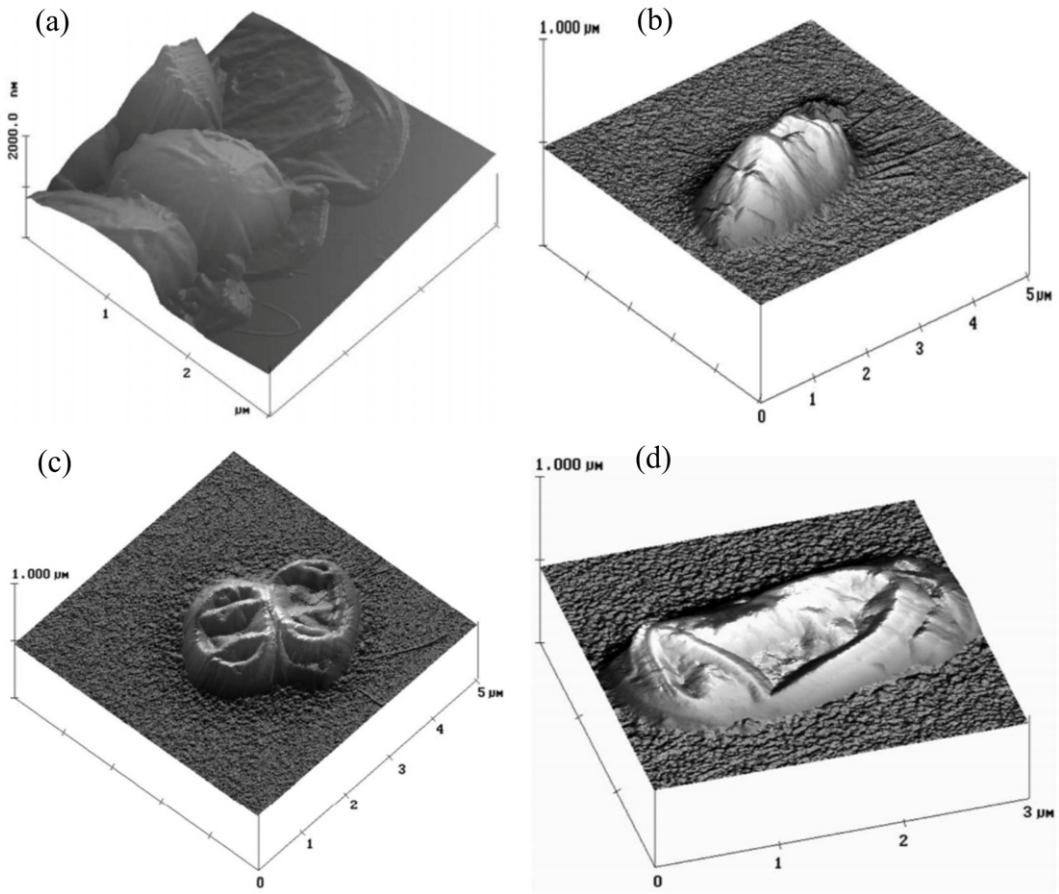

Figure 17. (*a*) AFM image of untreated *Bacillus cereus* (genetically similar to *Bacillus anthracis*), (*b*) after 2 s of plasma treatment, (*c*) 4 s, (*d*) 8 s, measured with atomic force microscopy [196].

(human tissues) is represented by the forced electrophoretic extraction of their cytoplasm, whose genetic material is not protected by a nuclear membrane like in eukaryotes. More complicated pathways are also possible. Studies on electrophoration of the cell membrane [198, 199] with microsecond-long discharges ($\sim$20 μs at 0.3–0.9 MV m^{-1}) have shown that electrophoration induces a rearrangement of the lipid bilayer of the cell membrane and the attachment of the two layers in a contiguous membrane at the site of pore formation. At that point, free Brownian motion allows the translocation of individual lipid molecules from one side of the membrane to the other side [200]. The externalization of phosphatidylserine (PS), a phospholipid component of the inner leaflet of the cell membrane, is then made possible. The externalization of PS acts as an important physiological signal, since cells with exposed PS are marked for phagocytosis and disposal. Nanosecond pulsed discharges (<300 ns) do not induce a significant poration of the cell membrane. However, PS externalization has also been observed in nanosecond discharges [201]. Mechanisms different from the microsecond-long pulses occur for nanosecond discharges. Pulses shorter than the charging time constant of the cell membrane (of the order of 100 ns) can penetrate across the cell membrane and porate the membranes of internal organelles such as mitochondria, nucleus, etc [202]. The fundamental difference of nanosecond-long pulses with respect to shorter discharges is evidenced not only by the permeabilization of intracellular granules, but also by a number of other phenomena not occurring in microsecond or longer discharges, such as calcium bursts [203], DNA damage [204], decoupling of the cytoskeleton from the plasma membrane (bleb formation) [205], cell death [206–208], melanoma growth inhibition [207, 209].

Computational investigations [210] on the application of cold non-thermal atmospheric-pressure plasmas to human tissue have evidenced the active role of energetic ions on the outer membrane of the cells. Kinetically energetic pulsed ions (<100 eV) produced in a cold plasma source at atmospheric pressure have an active role in delivering energy to the treated tissue. Furthermore, molecular dynamics of plasma ions impacting on lipid films at the same energies are responsible for sputtering yields of carbon atoms ranging from 1.0 to 10.

The rapid, selective and reliable destruction of pathogen agents on living tissues using atmospheric-pressure plasmas can be of major help to physicians, and lead towards large cuts in hospital costs. A number of critical unsolved issues have to be addressed before these new techniques can turn into operative systems in use at healthcare providers. It is currently not clear whether plasma treatment really kills the bacteria or simply inactivates them. It is also unclear whether a plasma treatment can be as effective on multi-layered bacteria colonies as it is on single-layer colonies. Furthermore,

bacteria are not the only infectious agents which must be removed for an effective sterilization. Other pathogens such as viruses and proteinaceous matter (prions, proteins, etc) have highly infectious potential and must be removed during the disinfection. The standard sterilization procedures of hospital tools, usually done in autoclave, are very effective in removing all kinds of infections agents and washing off large quantities of tissue fragments from medical instruments. An equivalent treatment using plasmas has to be able to efficiently remove both bacteria and all other kinds of pathogens. Unfortunately, plasma sterilization on viruses and prions has not been addressed as well as for bacteria. Only recently has the use of cold atmospheric plasmas been under investigation as a strategy for prion inactivation [210–212]. A He–O_2 atmospheric-pressure plasma jet has proven to be effective in the reduction of the quantity of model proteins (Bovine Serum Albumin) dry-deposited on SS substrates [213, 214]. The effectiveness on body tissue has not been tested yet. In most practical cases, prions and viruses happen to be in aqueous solution. Observing the degradation of prions and proteinaceous material in aqueous solution is intrinsically more difficult, due both to complications in the diagnostics and the more complex physicochemical processes involved, obstructing the reliability and the repeatability of the results. Few cases have been reported to date, and more investigations are undergoing. As relevant examples, recombinant green fluorescent protein (GPF) can be inactivated in *Escherichia coli* cells [215] thanks to a plasma treatment. Active plasma modification of the genetic structure of DNA has been observed [216, 217]. Plasma modification of bio-macromolecules in aqueous solutions and the consequent complex chemical activation of active species is currently lacking fundamental theoretical understanding. Deeper studies will be necessary in the future to address those critical important issues.

10. Summary

Recent development in vacuum-based sciences has been reviewed. Novel optical interferometer cavity devices for pressure standards allow for precise pressure measurements with ppm accuracy. Ultra-fast gauges enable determination of pressure changes at 10 ms resolution. Advanced simulation techniques improve understanding of gas–solid interactions and results are used in construction of huge ultra-high vacuum chambers such as RIHC, LIER, LHC, FAIR and ITER. Improved methods for gas dynamic simulations, interaction of gaseous molecules with solid surfaces as well as precise methods for gas sensing will contribute to optimization of future large vacuum facilities and thus solving the key problem—assuring reliable energy sources for future generations.

Novel methods, elaborated for describing accurately near-surface energy loss processes and simulating electron-, photon- and ion-induced electron spectra, have predicted new phenomena during surface excitations that reveal unknown details of electronic structure of new materials of great practical importance. Novel observations will influence understanding the plasmon oscillations and are considered a primary topic in application of gold nanoparticles used in sensing of biological materials. Complex application of surface analytical methods for studying chemical and structural properties of doped or functionalized carbon nanotubes or graphene layers lead to the development and production of new, highly effective catalysts of important chemical reactions, as well as to further exciting novel applications of these nanostructures in science and technology. Combination of various analytical techniques provides crucial information of structural modifications of cultural heritage objects, which in turn leads to development of reliable conservation techniques.

Research in the recently recognized field of biointrephases is of tremendously growing importance. Complementary methods such as XPS, SIMS and QCM have been applied successfully to study complex phenomena of interaction between biological materials and solid surfaces. The conformation of biomolecules is considered a major effect governing biological response and thus compatibility of materials for implants with neighbouring tissues. Open questions in this field of current interdisciplinary science abound and are often related to a lack of reliable analytical methods that operate at atmospheric pressure and in liquid environments.

Deposition of thin films using vacuum techniques is an established technology with numerous applications. The current trend is development of nanostructured films with functional properties. Modern sources of nanoparticles often apply evaporation or sputtering materials into a chamber of relatively high pressure of inert gas (∼10–100 Pa) and nanoparticles are created by homogeneous nucleation. Nanoparticles are then dragged by the buffer gas and exit the aggregation chamber through an orifice into a deposition chamber. Such systems are commonly equipped with mass filters to produce nanoparticles with very narrow size distributions. Future applications of this technique include development of novel scaffolds of functional properties.

Plasma nanoscience is one of the fastest growing fields of interdisciplinary research. Treatment of solid materials with appropriate gaseous plasma allows for synthesis of almost any material in the form of nanowires, nanospikes, nanotips, quantum dots and more complex shape. The technique allows for synthesis of large quantities of such materials and is thus expected to become a major technology for massive production of nanoparticles for industrial application, thus partially replacing ecologically unsuitable wet chemical methods.

Recent advances in plasma medicine have been reviewed. Gaseous plasma is successfully applied either for modification of functional properties of materials likely to come in contact with biological tissues or for treatment of tissues themselves. The first approach is particularly useful for improving the biocompatibility of vascular grafts as well as materials for wound dressings, while the second one is one of the most promising techniques for curing diabetes wounds and cancer. High electric fields occurring locally when treating tissues with localized atmospheric plasma sources as well as abundance of temporally limited charged particles interact selectively with biological cells causing apoptosis. Since the exact

mechanisms occurring at interaction between the plasma and cells is far from being well understood, tremendous progress in this interdisciplinary field is expected in the near future and extensive *in vivo* experiments are foreseen.

Acknowledgments

This work was partially supported by Slovenian Research Agency (grant #P2-0082), the Australian Research Council and CSIRO OCE Science Leadership Programme (Australia), Ministry of Science, Education and Sports of Croatia (grant #035-0352851-2856, #098-0982886-2895 and #098-0982886-2859), Grant Agency of the Czech Republic (grant #GACR 13-09853S), Ministry of Education, Youth and Sports of Czech Republic (grant #CZ.1.05/2.1.00/03.0111), Department of the Autonomous Province of Trento, New Széchenyi Plan (grant #TÁMOP-4.2.2.A-11/1/KONV-2012-0019 – the realization of this project is supported by the European Union, co-financed by the European Social Fund). Financial support from the German Federal Ministry of Economics and Technology (BMWi) through the programme Transfer von Forschungs- und Entwicklungsergebnissen (FuE) durch Normung und Standardisierung (TNS), and the European Union through the European Metrology Research Programme (EMRP) is highly appreciated. The EMRP is jointly funded by the EMRP participating countries within EURAMET and the European Union.

References

[1] Bacher J-P, Benvenuti C, Chiggiato P, Reinert M-P, Sgobba S and Brass A-M 2003 *J. Vac. Sci. Technol.* A **21** 167
[2] Nemanic V, Zajec B and Setina J 2001 *J. Vac. Sci. Technol.* A **19** 215
[3] Ishikawa Y and Nemanic V 2003 *Vacuum* **69** 501
[4] Stupnik A and Leisch M 2008 *Vacuum* **82** 170
[5] Malyshev O, Leisch M and de Segovia J *et al* 2010 *63rd IUVSTA Workshop on Surface Phenomena Limiting Ultimate Pressures in Vacuum Systems (Avila, Spain, Sept. 2010)*
[6] Benvenuti C and Francia F 1990 *J. Vac. Sci. Technol.* A **8** 3864
[7] Benvenuti C, Chiggiato P, Cicoira F, Aminot Y and Ruzinov V 2004 *Vacuum* **73** 139
[8] Malyshev O B, Middleman K J, Colligon J S and Valizadeh R 2009 *J. Vac. Sci. Technol.* A **27** 321
[9] Malyshev O B, Valizadeh R, Colligon J S, Hannah A, Middleman K J, Patel S and Vishnyakov V M 2009 *J. Vac. Sci. Technol.* A **27** 521
[10] Valizadeh R, Malyshev O B, Colligon J S, Hannah A and Vishnyakov V M 2010 *J. Vac. Sci. Technol.* A **28** 1404
[11] Malyshev O B, Valizadeh R and Hannah A 2014 *Vacuum* **100** 26
[12] Malyshev O B, Smith A P, Valizadeh R and Hannah A 2011 *Vacuum* **85** 1063
[13] Malyshev O B and Naran C 2012 *Vacuum* **86** 1363
[14] Hedlund E *et al* 2009 *Nucl. Instrum. Methods Phys. Res.* A **599** 1
[15] Hedlund E *et al* 2009 *J. Vac. Sci. Technol.* A **27** 139
[16] Kollmus H *et al* 2009 *J. Vac. Sci. Technol.* A **27** 245
[17] Malyshev O B, Zajec B, Haase A, Westerberg L, Leandersson M, Bender M, Krämer A, Kollmus H and Reich-Sprenger H 2010 *Vacuum* **85** 338
[18] Pearce R J H *et al* 2012 *Vacuum* **86** 1725
[19] Sharipov F 2013 *J. Vac. Sci. Technol.* A **31** 050806
[20] Malyshev O B 2012 *Vacuum* **86** 1669
[21] Malyshev O B and Cox M P 2012 *Vacuum* **86** 1692
[22] Babutzka M *et al* 2012 *New J. Phys.* **14** 103046
[23] Sharipov F and Seleznev V 1998 *J. Phys. Chem. Ref. Data* **27** 657
[24] Sharipov F 2011 *J. Phys. Chem. Ref. Data* **40** 023101
[25] Agrawal A and Prabhu S V 2008 *J. Vac. Sci. Technol.* A **26** 634
[26] Ketsdever A, Gimelshein N, Gimelshein S and Selden N 2012 *Vacuum* **86** 1644
[27] Frezzotti A, Ghiroldi G P and Gibelli L 2012 *Vacuum* **86** 1731
[28] Misdanitis S, Pantazis S and Valougeorgis D 2012 *Vacuum* **86** 1701
[29] Titarev V A and Shakhov E M 2012 *Vacuum* **86** 1709
[30] Sharipov F 2012 *Physica* A **391** 19723
[31] Graur I A, Polikarpov A P and Sharipov F 2012 *Z. Angew. Math. Phys.* **63** 503
[32] Sharipov F and Strapasson J L 2012 *Phys. Fluids* **24** 011703
[33] Kozak D V and Sharipov F 2012 *Brazilian J. Phys.* **42** 192
[34] Sharipov F and Graur I A 2012 *Vacuum* **86** 1778
[35] Varoutis S, Day C and Sharipov F 2012 *Vacuum* **86** 1952
[36] Sharipov F and Strapasson J L 2012 *Phys. Rev.* E **86** 031130
[37] Kalempa D and Sharipov F 2012 *Int. J. Heat Fluid Flow* B **30** 190
[38] Pantazis S, Valougeorgis D and Sharipov F 2013 *Vacuum* **97** 26
[39] Sharipov F 2012 *Vacuum* **86** 1697
[40] Gronych T, Jeřáb M, Peksa L, Wild J, Staněk F and Vičar M 2012 *Vacuum* **86** 1759
[41] Sharipov F and Strapasson J L 2013 *Phys. Fluids* **25** 027101
[42] Varoutis S and Day C 2012 *Fusion Eng. Des.* **87** 1395
[43] Luo X, Day C, Haas H and Varoutis S 2011 *J. Vac. Sci. Technol.* A **29** 041601
[44] Sengil N 2012 *Vacuum* **86** 1764
[45] www.nist.gov/pml/div685/grp01/plt-ims.cfm
[46] www.emrponline.eu/ www.ptb.de/emrp/vacuum.html
[47] Sonderegger K, Dür M, Buthig J, Sarantis P and Jousten K 2013 *J. Vac. Sci. Technol.* A **31** 060601
[48] Jousten K, Pantazis S, Buthig J, Model R, Wüest M and Iwicki J 2014 *Vacuum* **100** 14
[49] Sharipov F *et al* 2012 *Workshop on Measurement Characteristics and Use of Quadrupole Mass Spectrometers for Vacuum Applications (Bled, Slovenia)* www.ptb.de/emrp/ws-ind12- conferencescope.html
[50] Malyshev O B and Middleman K J 2008 *J. Vac. Sci. Technol.* A **26** 1474
[51] Ermakov A V and Hinch B J 2010 *Rev. Sci. Instrum.* **81** 013107
[52] Jousten K *et al* 2013 *Metrologia* **50** 07001
[53] Bergoglio M and Mari D 2012 *Measurement* **45** 2434
[54] Prazak D, Zuda J,Tesar J, Peksa L and Vicar M 2013 *Measurement* **46** 621
[55] Setina J, Avdiaj S and Erjavec B 2013 *Vacuum* **92** 20
[56] Li D, Cheng Y, Feng Y, Xi Z and Zhao L 2013 *Metrologia* **50** 15
[57] Werner W S M, Novák M, Salvat-Pujol F, Zemek J and Jiricek P 2013 Electron supersurface scattering on polycrystalline Au *Phys. Rev. Lett.* **110** 086110
[58] Pauly N and Tougaard S 2011 *Surf. Sci.* **605** 1556
[59] Salvat-Pujol F and Werner W S M 2011 *Phys. Rev.* B **83** 195416
[60] Stobinski L, Lesiak B, Kövér L, Tóth J, Biniak S, Trykowski G and Judek J 2010 *J. Alloys Compounds* **501** 77
[61] Turgeon S and Paynter R W 2001 *Thin Solid Films* **394** 44
[62] Mikolajczuk A, Borodzinski A, Stobinski L, Kedzierzawski P, Lesiak B, Kövér L, Tóth J and Lin H M 2010 *Phys. Status Solidi* b **247** 3063
[63] Lesiak B, Zemek J, Houdkova J, Jiricek P and Józvik A 2011 *J. Electron Spectrosc. Relat. Phenom.* **184** 360

[64] Tapasztó L, Dumitrica T, Kim S J, Nemes-Incze P, Hwang C and Biro L P 2012 *Nature Phys.* **8** 739
[65] Croveri P, Fragala I and Ciliberto E 2010 *Appl. Phys.* A **100** 927
[66] Alberghina M F, Barraco R, Brai M, Casaletto M P, Ingo G M, Marrale M, Policarpo D, Schillaci T and Tranchina L 2010 *Appl. Phys.* A **100** 953
[67] Fors Y, Jalilehvand F and Sandström M 2011 *Anal. Sci.* **27** 785
[68] Fors Y, Jalilehvand F, Risberg E D, Bjordal C, Philips E and Sandstorm M 2012 *J. Archaeological Sci.* **39** 2521
[69] Castner D G and Ratner B D 2002 *Surf. Sci.* **500** 26
Tirrell M *et al 2002 Surf. Sci.* **500** 61
Kasemo B 2002 *Surf. Sci.* **500** 656
Rod T H and Nørskov J K 2002 *Surf. Sci.* **500** 678
[70] Graf N, Gross T, Wirth T, Weigel W and Unger W 2009 *Anal. Bioanal. Chem.* **393** 1907
[71] Graf N, Yegen E, Gross T, Lippitz A, Weigel W, Krakert S, Terfort A and Unger W E S 2009 *Surf. Sci.* **603** 2849
[72] Min H, Girard-Lauriault P-L, Gross T, Lippitz A, Dietrich P and Unger W 2012 *Anal. Bioanal. Chem.* **403** 613
[73] Girard-Lauriault P-L, Dietrich P M, Gross T, Wirth T and Unger W E S 2013 *Plasma Process. Polym.* **10** 388
[74] Graf N, Yegen E, Lippitz A, Treu D, Wirth T and Unger W E S 2008 *Surf. Interface Anal.* **40** 180
[75] Funk C, Dietrich P M, Gross T, Min H, Unger W E S and Weigel W 2012 *Surf. Interface Anal.* **44** 890
[76] Hecht M, Fischer T, Dietrich P, Kraus W, Descalzo A B, Unger W E S and Rurack K 2013 *Chem. Open* **2** 25
[77] Dietrich P M, Horlacher T, Girard-Lauriault P-L, Gross T, Lippitz A, Min H, Wirth T, Castelli R, Seeberger P H and Unger W E S 2011 *Langmuir* **27** 4808
[78] Dietrich P M, Horlacher T, Girard-Lauriault P-L, Gross T, Lippitz A, Min H, Wirth T, Castelli T, Seeberger P H and Unger W E S 2011 *J. Carbohydr. Chem.* **30** 361
[79] Dietrich P M, Horlacher T, Gross T, Wirth T, Castelli R, Shard A G, Alexander M, Seeberger P H and Unger W E S 2010 *Surf. Interface Anal.* **42** 1188
[80] Oberleitner B, Dellinger A, Defforet M, Galtayries A, Castanet A-S and Semetey V 2013 *Chem. Commun.* **49** 1615
[81] Lhoest J-B, Detrait E, van den Bosch de Aguilar P and Bertrand P 1998 *J. Biomed. Mater. Res.* **41** 95
[82] Mar M N, Ratner B D and Yee S S 1999 *Sensors Actuators* B **54** 125
[83] Frateur I, Lartundo-Rojas L, Méthivier C, Galtayries A and Marcus P 2006 *Electrochem. Acta* **51** 1550
[84] Galtayries A, Warocquier-Clérout R, Nagel M-D and Marcus P 2006 *Surf. Interface Anal.* **38** 186
[85] Payet V, Dini T, Brunner S, Galtayries A, Frateur I and Marcus P 2010 *Surf. Interface Anal.* **42** 457
[86] Ray S and Shard A G 2011 *Anal. Chem.* **83** 8659
[87] Isaac J, Galtayries A, Kizuki T, Kokubo T, Berdal A and Sautier J-M 2010 *Euro. Cells Mater. J.* **20** 178
[88] Lefaix H, Galtayries A, Prima F and Marcus P 2013 *Colloids Surf.* A **439** 207
[89] Payet V, Brunner S, Galtayries A, Frateur I and Marcus P 2008 *Surf. Interface Anal.* **40** 215
[90] Choy K L 2003 *Prog. Mater. Sci.* **48** 57
[91] Mattox D M 2007 *Handbook of Physical Vapour Deposition (PVD) Processing* (Amsterdam: Elsevier)
[92] Siffalovic P *et al* 2011 *J. Appl. Crystallogr.* **43** 1431
[93] Hell J, Horkel M, Neubauer E and Eisenmenger-Sittner C 2010 *Vacuum* **84** 453
[94] Kumar A, Singh A, Samanta S, Debnath A K, Aswal D K and Gupta S K 2011 *Appl. Phys. Lett.* **99** 112102
[95] Vishnyakov V, Lu J, Eklund P, Hultman L and Colligon J 2013 *Vacuum* **93** 56
[96] Chappert C, Fert A and van Dau F N 2007 *Nature Mater.* **6** 813
[97] Awschalom D D and Flatté M E 2007 *Nature Phys.* **3** 153
[98] Paramês M L, Mariano J, Viskadourakis Z, Popovici N, Rogalski M S, Giapintzakis J and Conde O 2006 *Appl. Surf. Sci.* **252** 4610
[99] Viskadourakis Z, Paramês M L, Conde O, Zervos M and Giapintzakis J 2012 *Appl. Phys. Lett.* **101** 033505
[100] Rout S, Popovici N, Dalui S, Paramês M L, da Silva R C, Silvestre A J and Conde O 2013 *Curr. Appl. Phys.* **13** 670
[101] Dalui S, Rout S, Silvestre A J, Lavareda G, Pereira L C J, Brogueira P and Conde O 2013 *Appl. Surf. Sci.* **278** 127
[102] Das S, Singh R K, Dhar A, Ray S K, Anopchenko A, Daldosso N and Pavesi L 2011 *J. Appl. Phys.* **110** 024310
[103] Jabbour D E and Doderer D 2010 *Nature Photon.* **4** 604
[104] Konstantatos G and Sargent E H 2010 *Nature. Nanotechnol.* **5** 391
[105] Buljan M, Desnica U V, Dražić G, Ivanda M, Radić N, Dubcek P, Salamon K, Bernstorff S and Holy V 2009 *Phys. Rev.* B **79** 035310
[106] Buljan M *et al* 2013 *J. Nanopart. Res.* **15** 1485
[107] Buljan M, Roshchupkina O, Šantić A, Baehtz C, Muecklich A, Horak L, Vales V, Radić N, Bernstorff S and Grenzer J 2013 *J. Appl. Cryst.* **46** 709
[108] Buljan M, Radić N, Bernstorff S, Dražić G, Bogdanović-Radović I and Holý V 2012 *Acta Cryst.* A **68** 124
[109] Haberland H, Karrais M, Mall M and Thurner Y 1992 *J. Vac. Sci. Technol.* A **10** 3266
[110] Polonskyi O *et al* 2012 *Thin Solid Films* **520** 4155
[111] Drábik M *et al* 2011 *Plasma Process. Polym.* **8** 640
[112] Kylián O, Valeš V, Polonskyi O, Pešička J, Čechvala J, Solař P, Choukourov A, Slavínská D and Biederman H 2012 *Mater. Lett.* **79** 229
[113] Drábik M, Serov A, Kylián O, Choukourov A, Artemenko A, Kousal J, Polonskyi O and Biederman H 2012 *Plasma Process. Polym.* **9** 390
[114] Polonskyi O, Kylián O, Solař P, Artemenko A, Kousal J, Slavínská D, Choukourov A and Biederman H 2012 *J. Phys. D: Appl. Phys.* **45** 495301
[115] Kylián O, Polonskyi O, Kratochvíl J, Artemenko A, Choukourov A, Drábik M, Solař P, Slavínská D and Biederman H 2012 *Plasma Process. Polym.* **9** 180
[116] Solař P, Kylián O, Polonskyi O, Artemenko A, Arzhakov D, Drábik M, Slavínská D, Vandrovcová M, Bačáková L and Biederman H 2012 *Surf. Coat. Technol.* **206** 4335
[117] Meyyappan M, Delzeit L, Cassel A and Hash D 2003 *Plasma Sources Sci. Technol.* **12** 205
[118] Ostrikov K 2005 *Rev. Mod. Phys.* **77** 489
[119] Zheng J, Yang R, Xie L, Qu J, Liu Y and Li X 2010 *Adv. Mater.* **22** 1451
[120] Ostrikov K, Neyts E C and Meyyappan M 2013 *Adv. Phys.* **62** 113
[121] Iijima S 1991 *Nature* **354** 56
[122] Meyyappan M 2009 *J. Phys. D: Appl. Phys.* **42** 213001
[123] Ren Z F, Huang Z P, Xu J W, Wang J H, Bush P, Siegal M P and Provencio P N 1998 *Science* **282** 1105
[124] Merkulov V I, Melechko A V, Guillorn M A, Lowndes D H and Simpson M L 2001 *Appl. Phys. Lett.* **79** 2970
[125] Kato T and Hatakeyama R 2010 *ACS Nano* **4** 7395
[126] Volotskova O, Fagan J A, Huh J Y, Phelan F R, Shashurin A and Keidar M 2010 *ACS Nano* **4** 5187
[127] Kumar S, Mehdipour H and Ostrikov K 2013 *Adv. Mater.* **25** 69
[128] Ostrikov K and Mehdipour H 2011 *ACS Nano* **5** 8372
[129] Wang H and Ren Z F 2011 *Nanotechnology* **22** 405601
[130] Melechko A V, Merkulov V I, McKnight T E, Guillorn M A, Klein K L, Lowndes D H and Simpson M L 2005 *J. Appl. Phys.* **97** 041301
[131] Wang B B and Zhang B 2006 *Carbon* **44** 1949

[132] Levchenko I and Ostrikov K 2007 *J. Phys. D: Appl. Phys.* **40** 2308
[133] Seo D H, Kumar S and Ostrikov K 2011 *J. Mater. Chem.* **21** 16339
[134] Kato T and Hatakeyama R 2012 *Nature Nanotechnol.* **7** 651
[135] Xie L, Jiao L and Dai H 2010 *J. Am. Chem. Soc.* **132** 14751
[136] Elias D C *et al* 2009 *Science* **323** 610
[137] Seo D H, Rider A E, Kumar S, Randeniya L K and Ostrikov K 2013 *Carbon* **60** 221
[138] Ostrikov K, Cvelbar U and Murphy A B 2011 *J. Phys. D: Appl. Phys.* **44** 174001
[139] Cvelbar U, Chen Z, Sunkara M K and Mozetic M 2008 *Small* **4** 1610
[140] Cvelbar U, Ostrikov K and Mozetic M 2008 *Nanotechnology* **19** 405605
[141] Kumar V *et al* 2008 *J. Phys. Chem.* C **38** 237
[142] Sharma S and Sunkara M K 2002 *J. Am. Chem. Soc.* **124** 12288
[143] Filipič G and Cvelbar U 2012 *Nanotechnology* **23** 194001
[144] Chen Z *et al* 2008 *Chem. Mater.* **20** 3224
[145] Ostrikov *et al* 2010 *Nanoscale* **2** 2012
[146] Sunkara M K *et al* 2004 *J. Mater. Chem.* **14** 590
[147] Vaddiraju S *et al* 2005 *Nano Lett.* **5** 1625
[148] Hofmann S *et al* 2008 *Nature Mater.* **7** 372
[149] Mehdipour H and Ostrikov K, 2013 *J. Am. Chem. Soc.* **135** 1912
[150] Robertson J 2012 *J. Mater. Chem.* **22** 19858
[151] Meduri P *et al* 2009 *Nano Lett.* **9** 612
[152] Cvelbar *et al* 2012 *Appl. Phys. Lett.* **100** 243103
[153] Thangala J, Chen Z, Chin A and Ning C Z 2009 *Cryst. Growth Des.* **9** 3177
[154] Cvelbar U *et al* 2012 *Chem. Commun.* **48** 11070
[155] Cvelbar U 2011 *J. Phys. D: Appl. Phys.* **44** 174014
[156] Shiratani M, Koga K, Ando S, Inoue T, Watanabe Y, Nunomura S and Kondo M 2007 *Surf. Coat. Technol.* **201** 5468
[157] Rider A E, Ostrikov K and Levchenko I 2008 *Nanotechnology* **19** 355705
[158] Shiratani M, Koga K, Iwashita S, Uchida G, Itagaki N and Kamataki K 2011 *J. Phys. D: Appl. Phys.* **44** 174038
[159] Cheng Q, Tam E, Xu S and Ostrikov K 2010 *Nanoscale* **2** 594
[160] Uchida G *et al* 2012 *Japan. J. Appl. Phys.* **51** 01AD01
[161] Levchenko I *et al* 2013 *J. Phys. Chem. Lett.* **4** 681
[162] Vesel A, Kolar M, Doliska A, Stana-Kleinschek K and Mozetic M 2012 *Surf. Interface Anal.* **44** 1565
[163] Cvelbar U, Mozetic M, Hauptman N and Klanjsek-Gunde M 2009 *J. Appl. Phys.* **106** 103303
[164] Vrlinic T, Debarnot D, Legeay G, Coudreause A, Ee Moualij B, Zorzi W, Perret-Liaude A, Quadrio I, Mozetic M and Poncin-Eppaillard F and 2012 *Biointerphases* **7** 66
[165] Vrlinic T, Debarnot D, Legeay G, Coudreause A, Ee Moualij B, Zorzi W, Perret-Liaude A, Quadrio I, Mozetic M and Poncin-Eppaillard F 2012 *Macromol. Biosci.* **12** 830
[166] Popelka A, Novak I, Lehocky M, Junkar I, Mozetic M, Kleinova A, Jaginova I, Slouf M, Bilek F and Chodak I 2012 *Carbohydr. Polym.* **90** 1501
[167] Breitwieser D, Spirk S, Fasl H, Ehmann H, Chemelli A, Reichel V, Gspan C, Stana-Kleinschek K and Ribitsch V 2013 *J. Mater. Chem.* B **2013** 2022
[168] Junkar I, Cvelbar U and Lehocky M 2011 *Mater. Tehnol.* **45** 221
[169] Junkar I, Cvelbar U, Vesel A, Hauptman N and Mozetic M 2009 *Plasma Processes Polym.* **6** 667
[170] Cvelbar U, Junkar I and Modic M 2011 *Japan. J. Appl. Phys.* **50** 08JF02
[171] Modic M Junkar I, Vesel A and Mozetic M 2012 *Surf. Coat. Technol.* **213** 98
[172] Mozetic M, Vesel A, Stana-Kleinschek K and Persin Z 2011 *European Patent Office* EP11006735.2
[173] Persin Z, Devetak M, Drevensek-Olenik I, Vesel A, Mozetic M and Stana-Kleinschek K 2013 *Carbohydr. Polym.* **97** 143
[174] Heinlin J, Morfill G, Landthaler M, Stolz W, Isbary G, Zimmermann J L, Shimizu T and Karrer S 2010 *J. Deutsch. Dermatol. Gesellsc.* **8** 968
[175] Fridman G *et al* 2006 *Plasma Chem. Plasma Process.* **26** 425
[176] Watson J P *et al* 1997 *Gut* **40** 156
[177] Wahab P J, Mulder C J, den Hartog G and Thies J E 1997 *Endoscopy* **29** 176
[178] Dajcman D, Skalicky M, Pernat C and Pocajt M 2001 *Wien Klin Wochenschr.* **113** 39
[179] Vargo J J 2004 *Gastrointestinal Endoscopy* **59** 81
[180] Raiser J and Zenker M 2006 *J. Phys. D: Appl. Phys.* **39** 3520
[181] Rabenstein T, May A, Michel J, Manner H, Pech O, Gossner L and Ell C 2007 *Endoscopy* **39** 141
[182] Morrison J C F 1977 Electrosurgical method and apparatus for initiating an electrical discharge in an inert gas flow *US Patent* 4,040,426
[183] Laroussi M 1996 *IEEE Trans. Plasma Sci.* **24** 1188
[184] Anderson K M *et al* 1999 *Med. Hypotheses* **52** 451
[185] Birmingham, J G and Hammerstrom D J 2000 *IEEE Trans. Plasma Sci.* **28** 51
[186] Soloshenko I A *et al* 2000 *Plasma Phys. Rep.* **26** 792
[187] Efremov N M *et al* 2000 *IEEE Trans. Plasma Sci.* **28** 238
[188] Moisan M *et al* 2002 *Pure Appl. Chem.* **74** 349
[189] Kieft I E *et al* 2004 *Bioelectromagnetics* **25** 362
[190] Sladek R E J and Stoffels E 2005 *J. Phys. D: Appl. Phys.* **38** 1716
[191] Cvelbar U *et al* 2006 *J. Phys. D* : *Appl. Phys.* **39** 3487
[192] Laroussi M *et al* 2006 *Plasma Process. Polym.* **3** 470
[193] Kuo S P *et al* 2006 *IEEE Trans. Plasma Sci.* **34** 1275
[194] Goree J *et al* 2006 *IEEE Trans. Plasma Sci.* **34** 1317
[195] Fridman A, Chirokov A and Gutsol A 2005 *J. Phys. D: Appl. Phys.* **38** R1
[196] Tarasenko O, Nourbakhsh S, Kuo S P, Bakhtina A, Alusta P, Kudasheva D, Cowman M and Levon K 2006 *IEEE Trans. Plasma Sci.* **34** 1281
[197] Weaver J C 1995 *The Biomedical Engineering Handbook* ed J D Bronzino (Boca Raton, FL: CRC) pp 1431–40
[198] Dressler V, Schwister K, Haest C W M and Deuticke B 1983 *Biochim. Biophys. Acta.* **732** 304
[199] Haest C W M, Kamp D and Deuticke B 1997 *Biochim. Biophys. Acta.* **1325** 17
[200] Sonnleitner A, Schutz G J and Schmidt T 1999 *Biophys. J.* **77** 2638
[201] Vernier P T, Sun Y, Marcu L, Craft C M and Martin A 2004 *Biophys. J.* **86** 4040
[202] Schoenbach K H, Beebe S J and Buescher E S 2001 *Bioelectromagnetics* **22** 440
[203] Vernier P T, Sun Y, Marcu L, Salem S, Craft C M and Gundersen M A 2003 *Biochem. Biophys. Res. Commun.* **310** 286
[204] Stacey M, Stickley J, Fox P, Statler V, Schoenbach K, Beebe S J and Buescher S 2003 *Mutat. Res.* **542** 65
[205] Pakhomov A G, Kolb J, Shevin R, White J, Joshi R P and Schoenbach K S 2007 *Arch. Biochem. Biophys.* **465** 109
[206] Beebe S J, Fox P M, Rec L J, Willis E L and Schoenbach K H 2003 *FASEB J.* **17** 1493
[207] Beebe S J, Fox P M, Rec L J, Somers K, Stark R H and Schoenbach K H 2002 *IEEE Trans. Plasma Sci.* **30** 286
[208] Pakhomov A G, Phinney A, Ashmore J, Walker K, Kolb J F, Kono S, Schoenbach K S and Murphy M R 2004 *IEEE Trans. Plasma Sci.* **32** 1579

[209] Nuccitelli R, Pliquett U, Chen X, Ford W, James Swanson R, Beebe S J, Kolb J F and Schoenbach K H 2006 *Biochem. Biophys. Res. Commun.* **343** 351
[210] Bayliss D L, Walsh J L, Shama G, Iza F and Kong M G 2009 *New J. Phys.* **11** 115024
[211] Julak J, Janouskova O, Scholtz V and Holada K 2011 *Plasma Process. Polym.* **8** 316
[212] Takai E, Kitano K, Kuwabara J and Shiraki K 2012 *Plasma Process. Polym.* **9** 77
[213] Deng X T, Shi J J and Kong M G 2007 *J. Appl. Phys.* **101** 074701
[214] Deng X T, Shi J J, Chen H L and Kong M G 2007 *Appl. Phys. Lett.* **90** 013903
[215] Yasuda H, Hashimoto M, Rahman M M, Takashima K and Mizuno A 2008 *Plasma Process. Polym.* **5** 615
[216] Li G, Li H-P, Wang L-Y, Wang S, Zhao H-X, Sun W-T, Xing X-H and Bao C-Y 2008 *Appl. Phys. Lett.* **92** 221504
[217] Yan X *et al* 2009 *Appl. Phys. Lett.* **95** 083702